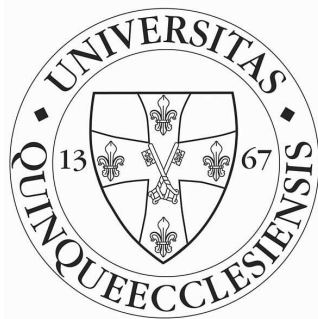# INVESTIGATION OF POTENTIAL PHARMACOLOGICAL DRUG TARGETS IN THE DEVELOPMENT AND PROGRESSION OF HYPERTENSIVE ORGAN DAMAGES

PhD thesis

Author: Laszlo Deres

Program leader: Prof. Kalman Toth M.D., Ph.D., Sc.D.

Project leader: Robert Halmosi M.D., Ph.D.

First Department of Medicine
University of Pécs, Medical School
Hungary

2014

Contents

1. ABBREVIATIONS

AKT	protein kinase B (PKB)
BNP	B-type natriuretic peptide
BW	body weight
DAP	diastolic arterial blood pressure
EF	ejection fraction
ERK ½	extracellular signal-regulated kinase
FS	fractional shortening
GSK-3β	glycogen synthase kinase-3β
HF	heart failure
IMT	intima-media thickness
IR	ischemia-reperfusion
IVS (d)	thickness of interventricular septum in diastole
IVS (s)	thickness of interventricular septum in systole
JNK	c-jun N-terminal kinase
LVEDV	left ventricular end-diastolic volume
LVESV	left ventricular end-systolic volume
LVID (d)	left ventricular end-diastolic diameter
LVID (s)	left ventricular end-systolic diameter
MAP	mean arterial blood pressure
MAPK	mitogen activated protein kinase
NAD+	nicotinamide adenine dinucleotide
NIH	National Institute of Health
NSAID	non-steroidal anti-inflammatory drug
PARP	poly(ADP-ribose) polymerase
PI3K	phosphatidylinositol-3-kinase
PKC	protein kinase C
PW (d)	thickness of left ventricular posterior wall in diastole
PW (s)	thickness of left ventricular posterior wall in systole
ROS	reactive oxygen species
RWT	relative wall thickness
SAP	systolic arterial pressure
SEM	standard error of the mean
SHR	spontaneously hypertensive rat

SPB	systolic blood pressure
TBS	TRIS-buffered saline
TGF-β	transforming growth factor-β
TL	lenght of right tibia
WKY	Wistar-Kyoto rat
WV	weight of ventricles

2. INTRODUCTION

Hypertension is a major public health problem both in middle-aged and in elderly people. It is both a complex disease and an important risk factor for other cardiovascular outcomes, such as sudden cardiac death, stroke, myocardial infarction, heart failure, and renal diseases (1). Unfortunately, the control of arterial hypertension is far from optimal and has improved only minimally over the last decades (1). Side effects of antihypertensive drugs, complaints due to their blood pressure lowering effect and inadequate compliance are the key factors in the background of inadequate control of hypertension (1,2). Moreover lowering blood pressure to the optimal range can be harmful in elderly patients (3,4). In order to optimize management of hypertension, some recent efforts focus on protecting the heart and the vasculature from hypertension induced remodeling with or without lowering the blood pressure (5).

2.1. Experimental model of chronic hypertension

SHR have been widely used as a model for hypertensive heart disease and hypertension induced vascular remodeling (6,7). The SHR was originally introduced by Okamoto and Aoki as a model of genetic hypertension. The progression of hypertrophy and impaired cardiac function in the SHR is similar to the clinical course of patients with hypertension. Persistent hypertension develops in the SHR after approximately 6 weeks of age. Following a relatively long period of stable hypertension and compensated hypertrophy, at approximately 18 months of age, animals begin to develop evidence of impaired function (tachypnea, labored respiration) (8,9).

The development of vascular remodeling is an early and important consequence of hypertension. Vascular remodeling is mainly characterized by vascular smooth muscle cell hypertrophy and increased production of extracellular matrix (10). Remodeling is initially an adaptive process that evolves in response to long-term pressure overload, but finally it can contribute to the development of hypertensive target organ damages (10,11).

2.2. Cell signaling mechanisms in hypertension

A number of physiological, pharmacological and pathological stimuli initiate cardiac hypertrophy (12). In addition, cardiac hypertrophy is associated with alterations in intracellular signaling transduction pathways, including alterations of G-protein-coupled receptors, small G protein, mitogen activated protein kinase (MAPK), protein kinase C (PKC), calcineurin and calmodulin and so on. Various signaling pathways are involved in the complicated interactions that finally promote cardiac hypertrophy and HF (13).

Growing evidences suggest that normal cardiac growth and exercise-induced hypertrophy are primarily regulated by the PI3K/Akt pathway. Many pro-hypertrophic stimuli have been shown to activate the serine/threonine kinase Akt, and PI3K-activation is an important common step in this process. Of the 3 Akt genes, only Akt-1 and -2 are expressed at substantial levels in the heart (14). Akt has two downstream targets: mammalian target of Rapamycin (mTOR) and Glycogen synthase kinase 3β (GSK-3β) (15, 16). Recent studies revealed an important role for Akt-signaling in cardiac angiogenesis. Ineffective angiogenesis however might contribute to the transition from hypertrophy to HF (14). The activity of GSK-3β is controlled by the phosphorylation status of serine-9. Several protein kinases, including Akt, inactivate GSK-3 β by phosphorylation of serine-9 (12, 14, 15,).

Growing data suggest that modulation of the complex network of MAPK cascades could be a rewarding approach to treat cardiomyocyte hypertrophy and HF (12,14). The MAPKs are elements of three-tiered protein kinase cascades and comprise basically three subfamilies, the extracellular signal-regulated kinases (ERKs), c-jun N-terminal kinases (JNKs) and the p38 MAPKs. While the ERKs are particularly implicated in growth-associated responses, the latter two groups are generally activated by cytotoxic stress factors (14). Protein kinase C (PKC) is critically involved in the development of cardiac hypertrophy and HF. Furthermore, the data suggest also that individual PKC isoforms have different effects on signaling pathways, variously leading to changes in cardiac contractility, hypertrophic response, and tolerance to myocardial ischemia in the heart (13).

By now it has been well established that oxidative stress has a causative role in the development of hypertensive vascular complications and vascular remodeling (10,17). ROS are important in regulating endothelial function and vascular tone, and are implicated in endothelial dysfunction, inflammation, hypertrophy, apoptosis, migration, fibrosis and angiogenesis (18,19). Oxidative stress induced signaling such as activation of MAPKs, PKC isoenzymes, NF-κB, AP-1 and STAT can significantly contribute to the development of hypertension induced vascular remodeling (20,21–23).

Recent studies revealed an important role for transforming growth factor-β (TGF-β) and SMAD2 signaling in multiple cardiovascular diseases, including hypertension, restenosis, atherosclerosis, cardiac remodeling and hypertrophy and heart failure (24,25).

TGF-β has long been believed to be the most important ECM regulator. Cardiac fibrosis is thought to be partially mediated by TGF-β1, a potent stimulator of collagenproducing cardiac fibroblasts (26,17). TGF-β reduces collagenase production and stimulates the expression of tissue inhibitor of metalloproteinases (TIMP), (26,27).

TGF-β predominantly transmits the signals through cytoplasmic proteins called Smads, which translocate into the cell nucleus acting as transcription factors. Smad proteins are expressed in VSMC and mediate TGF-β signaling (28). In VSMC, TGF-β1 increases phosphorylation of Smad2 and Smad3, which form heterotrimers with Smad4. This complex translocates into the nucleus, binds to Smad-related DNA sequences and increases the transcription of genes involved in vascular fibrosis such as fibronectin, type I collagen and connective tissue growth factor (CTGF) (28).

2.3. Cardiovascular effects of PARP inhibition

It is known that activation of poly(ADP-ribose) polymerase enzyme (PARP) plays an important role in the development of postinfarction as well as long-term hypertension induced heart failure. The poly(ADP-ribose) polymerase (PARP) enzyme becomes activated in response to DNA single-strand breaks that can be excessive as a response to free radicals and oxidative cell damage. PARP is an energy-consuming enzyme that transfers ADP-ribose units to nuclear proteins. As a result of this process, the intracellular NAD^+ and ATP levels decrease remarkably resulting in cell dysfunction and cell death via the necrotic route. Therefore, PARP-activation contributes to the pathogenesis of various cardiovascular diseases including endothelial dysfunction, ischemia-reperfusion injury and myocardial infarction, as well as HF. Several studies reported that endothelial dysfunction associated with hypertension also depends on PARP activity and can be prevented by its pharmacological inhibition (29, 30).
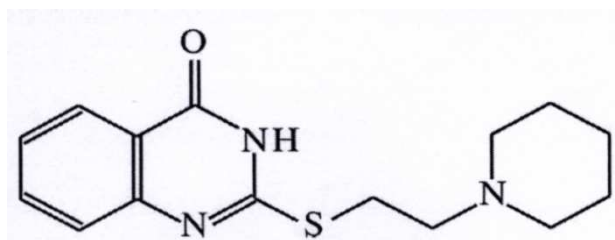
Figure 1. Chemical structure of L-2286 (2-[(2-Piperidine-1-ylethyl)thio]quinazolin-4(3H)-one).

It has been shown previously that our experimental agent, an isoquinoline derivative PARP-inhibitor, L-2286 (Fig. 1) had beneficial effects against oxidative cell damage, ischemia-reperfusion injury and against the development of postinfarction or long-term high blood pressure-induced heart failure. Although the molecule has a slight scavenger characteristic, its forementioned effects were mediated mainly by influencing the Akt-1/GSK-3β, MAPK and PKC signal transduction factors (31, 32, 33).

2.4. Importance of bradykinin B1 receptor antagonism

Hypertension is a public health problem mainly in middle-aged and in elderly people. Several studies showed that increasing levels of SBP were associated with a higher risk of cerebro- and cardiovascular events. One important factor in the background of the inadequate hypertension control is the drug interactions between antihypertensive agents and several non-cardiovascular drugs e.g. analgetics, such as NSAIDs (37,38).

NSADs are the most widely used analgetics nowadays. Unfortunately all of them increase markedly the cardiovascular mortality and morbidity. Therefore we considered it important to monitor the cardiovascular effects of a novel analgetic agent, bradykinin B1 receptor antagonist. According to several previous works, bradykinin B1 receptor antagonists may have beneficial effects in some cardiovascular diseases.

Kinins are biologically active peptides that exert a broad spectrum of physiological effects, including vasodilation, inflammation, and pain induction (39). The biological effects of kinins are mediated through the stimulation of bradykinin B1 and B2 receptors. The B2 receptor is constitutively expressed and is activated by intact kinins, bradykinin, and kallidin. This receptor is believed to play an important role in mediating the beneficial effects of ACE-

inhibitors, but it is also involved in the acute phases of inflammation (39-41). However the B1 receptor is activated by the carboxypeptidase metabolites of kinins, des-Arg9-BK and des-Arg10-kallidin. The B1 receptor is normally weakly expressed, but it is upregulated in the presence of cytokines and endotoxins or during tissue injury (39-41). The B1 receptor participates in chronic inflammation and pain (37-41); thus, bradykinin B1 receptor antagonists are a potentially novel approach for treating these conditions without having deleterious cardiovascular effects.

.

3. AIMS OF THE STUDY

3.1.

Our present study aimed to clarify whether pharmacological PARP-inhibition has protective effect in an SHR model against the development of the early stage of hypertensive cardiac remodeling.

-The aim of this work was to provide evidence for new molecular mechanisms of the cardioprotective effect of PARP inhibition.

-We estimated its effect on cardiac fibrosis.

-We tested whether PARP inhibition had beneficial effect on signal transduction pathways taking part in cardiac remodeling.

3.2.

In the second experiment we investigated the effects of the bradykinin B1 receptor antagonist test substance, FGY-1153 on the development of hypertensive organ damages in spontaneously hypertensive rats (SHR).

- We tried to examine the effect of bradykinin B1 receptor antagonism on body weight, food consumption and blood pressure.

- We tried to examine the effect of bradykinin B1 receptor antagonism on hypertension induced cardiovascular remodeling (intima media thickness, interstitial fibrosis, LVHT).

- We tested whether bradykinin B1 receptor antagonist had beneficial effect on signal transduction pathways taking part in cardiac remodeling.

4. THE EFFECT OF PARP INHIBITION IN CARDIAC REMODELING

4.1. Materials and methods

4.1.1. Ethics Statement

The investigation conforms to the Guide for the Care and Use of Laboratory Animals published by the U.S. National Insitutes of Health (NIH Publication No. 85-23, revised 1996), and was approved by the Animal Research Review Committee of the University of Pecs, Medical School.

4.1.2. Experimental protocol

Six week old male WKY-strain Wistar Kyoto and spontaneously hypertensive rats (Charles River Laboratories, Budapest, Hungary) were used. Animals were kept under standard conditions throughout the experiment; 12 h light-dark cycle, water and rat chow provided ad libitum. SHRs were randomly divided into two groups; SHR-L and SHR-C. SHR-L group was treated with L-2286 (2-[(2-piperidin-1-ylethyl)thio]quinazolin-4(3H)-one), a water-soluble PARP-inhibitor (5 mg/b.w. in kg/day, n=12), while SHR-C group received only placebo (n=11, SHR-C) p. os for 24 weeks. WKY rats were used as age-matched controls (n=10). Dosage of L-2286 administered in drinking water was based on preliminary data about the volume of daily consumption (32). At the beginning and at the end of the 24-week-long period, echocardiographic measurements were performed. Invasive blood pressure measurements were carried out on 3 rats of each group at the end of the study. These rats were anesthetized with ketamine hydrochloride (Richter Gedeon Ltd., Budapest, Hungary) intraperitoneally and a polyethylene catheter (Portex, London, UK) was inserted into their left femoral artery. Systolic, diastolic and mean arterial blood pressure was determined by CardioMed System CM-2005 (Medi-Stim AS, Oslo, Norway). Animals were euthanized with an overdose of ketamine hydrochloride intraperitoneally and heparinized with sodium heparin (100 IU/rat i.p., Biochemie GmbH, Kundl, Austria). After the sacrifice, blood was collected to determine the concentration of plasma brain-derived natriuretic peptide (BNP), and hearts were removed, the atria and great vessels were trimmed from the ventricles and weight of the ventricles was measured, which was then normalized to body mass (index of cardiac

hypertrophy). The lung wet weight-to-dry weight ratio (an index of pulmonary congestion) was also measured in 7-9 experimental animals. Hearts were freeze-clamped and were stored at -70°C or fixed in 10% formalin. In order to detect the extent of fibrotic areas, histologic samples were stained with Masson's trichrome. The phosphorylation state of Akt-1/GSK-3β, MAPK and PKC signaling molecules were monitored by Western blotting.

4.1.3. *Determination of plasma B-type natriuretic peptide*

Blood samples were collected into Lavender Vacutainer tubes containing EDTA and aprotinin (0.6 IU/ml of blood), and were centrifuged at 1600 g for 15 minutes at 4°C to separate the plasma. Supernatants were collected and kept at -70°C. BNP-45 were determined by enzyme immunoassay method as the manufacturer proposed (BNP-45, Rat EIA Kit, Phoenix Pharmaceuticals Inc., CA, USA).

4.1.4. *Histology*

Ventricles fixed in formalin were embedded in paraffin, and 5 μm thick sections were cut from base to apex. Sectiones were stained with Masson's trichrome staining to detect the interstitial fibrosis, and quantified by the NIH ImageJ image processing program as described previously (31).

4.1.5. *Western blot analysis*

Fifty milligrams of heart samples were homogenized in ice-cold 50 mM Tris buffer, pH 8.0 containing protease inhibitor cocktail 1:100, and 50 mM sodium vanadate (Sigma-Aldrich Co., Budapest, Hungary), and were harvested in 2x concentrated sodium dodecyl sulphate (SDS)-polyacrylamide gel electrophoresis sample buffer. Proteins were separated on 10% or 12% SDS-polyacrylamide gel and transferred to nitrocellulose membranes. After blocking (2 h with 3% nonfat milk in Tris-buffered saline), membranes were probed overnight at 4°C with primary antibodies recognizing the following antigenes: phospho-specific Akt-1/protein kinase B-α Ser^{473} (1:1000), Actin (1:10000), phospho-specific glycogen synthase kinase (GSK)-3β Ser^9 (1:1000), phospho-specific extracellular signal-regulated kinase (ERK

1/2) Thr^{202}-Tyr^{204} (1:1000), phospho-specific p38 mitogen-activated protein kinase (p38-MAPK) Thr^{180}-Gly-Tyr^{182} (1:1000), phospho-specific c-Jun N-terminal kinase (JNK) Thr^{183}-Tyr^{185} (1:1000), phospho-specific protein kinase C (PKC) (pan) βII Ser^{660} (1:1000), phospho-specific protein kinase C α/βII (PKC α/βII) Thr$^{638/641}$ (1:1000), phospho-specific protein kinase C δ (PKC δ) Thr^{505} (1:1000), phospho-specific protein kinase C ζ/λ (PKC ζ/λ) Thr$^{410/403}$ (1:1000), phospho-specific protein kinase C ε (PKC ε) Ser^{729} (1:1000), anti-poly(ADP-ribose) (anti-PAR, 1:5000), phospho-Foxo1A (forkhead transcription factor, FKHR Ser^{256}, 1:1000), Heat shock protein 72 (Hsp72, 1:20000), Heat shock protein 90 (Hsp90, 1:1000). Antibodies were purchased from Cell Signaling Technology (Beverly, MA, USA) except from actin, which was bought from Sigma-Aldrich Co, (Budapest, Hungary), phospho-specific PKC ε, which was purchased from Upstate (London, UK), anti-PAR, which was purchased from Alexis Biotechnology (London, UK), Hsp90, which was bought from Santa Cruz Biotechnology (Wembley, UK), Hsp72, which was purchased from StressGene Biomol GmbH (Hamburg, Germany). Membranes were washed six times for 5 min in Tris-buffered saline, pH 7.5 containing 0.2% Tween before addition of goat anti-rabbit horseradish peroxidase-conjugated secondary antibody (1:3000 dilution, Bio-Rad, Budapest, Hungary). The antibody-antigen complexes were visualized by means of enhanced chemiluminescence. After scanning, results were quantified by NIH ImageJ program. Pixel densities of bands were normalized to that of the loading controls.

4.1.6. *Noninvasive evaluation of cardiac functions and dimensions*

At the start of the experiment, all animals were examined by echocardiography to exclude rats with any heart abnormalities. Transthoracic two-dimensional echocardiography was performed under inhalation anesthesia at the beginning of the experiment and on the day of sacrifice. Rats were lightly anesthetized with a mixture of 1.5% isoflurane (Forane, Abbott Laboratories, Hungary) and 98.5% oxygen. The chest of animals was shaved, acoustic coupling gel was applied and warming pad was used to maintain normothermia. Rats were imaged in the left lateral decubitus position. Cardiac dimensions and functions were measured from short- and long-axis views at the mid-papillary level by a VEVO 770 high-resolution ultrasound imaging system (VisualSonics, Toronto, Canada) equipped with a 25 MHz transducer. LV fractional shortening (FS), ejection fraction (EF), LV end-diastolic volume (LVEDV), LV end-systolic volume (LVESV), and the thickness of septum and posterior wall

were determined. FS (%) was calculated by $100 \times ((LVID_d-LVID_s)/LVID_d)$ (LVID: LV inside dimension; d: diastolic; s: systolic), EF (%) was calculated by $100 \times ((LVEDV-LVESV)/LVEDV)$, relative wall thickness (RWT) was calculated by (PW thickness + interventricular septal thickness)/$LVID_d$.

4.1.7. Statistical analysis

All data are expressed as mean±SEM. First of all the homogeneity of the groups was tested by F-test (Levene's test). There were no significant differences among the groups. Comparisons among groups were made using one-way ANOVA (SPSS for Windows 11.0). For post hoc comparison Bonferroni test was chosen. Values of $p < 0.05$ were considered statistically significant.

4.2. Results

4.2.1. *Effect of PARP inhibition on gravimetric parameters of spontaneously hypertensive rats*

Body weights did not differ significantly among the three groups (WKY: 71.01±0.11 g, SHR-C: 72.03±2.36 g, SHR-L: 69.92±3.21 g, 6-week-old rats) at the beginning of our study. However, at the end of the 24-week-long treatment period, body weights of WKY group were significantly higher than those of SHR-C and SHR-L groups (WKY: 392.7±14.01 g, SHR-C: 323.8±11.27 g, SHR-L: 321.9±6.84 g, p<0.01 WKY vs. SHR groups, 30-week-old rats). The degree of myocardial hypertrophy was determined by ventricular weight to body weight ratio (WV/BW, mg/g). This parameter was significantly increased in SHR groups compared to the WKY group (WV/BW: WKY: 2.95±0.17, SHR-C: 4.48±0.12, SHR-L: 3.85±0.15, p<0.05 WKY vs. SHR groups). Similar results were obtained in case of weights of ventricles (WV, WKY: 1.16±0.17 g, SHR-C: 1.45±0.18 g, SHR-L: 1.24±0.24 g, p<0.05 WKY vs. SHR groups). The WV and WV/BW ratios were significantly decreased by L-2286 treatment (p<0.05 SHR-L vs. SHR-C). The lung wet weight-to-dry weight ratio was not elevated significantly in SHR-C and SHR-L compared to WKY groups (Table 1). All these results indicate the presence of cardiac hypertrophy without congestive heart failure in the SHR-C group that was ameliorated in the SHR-L group.

	WKY	SHR-C	SHR-L
BW[6w] (g)	71.01±1.89	72.02±2.36	69.9±3.21
BW (g)	393±14.01	323.8±11.27[a]	321.86±6.8[a,c]
WV (g)	1.16±0.17	1.45±0.18[b]	1.24±0.24[b,c]
WV/BW (mg/g)	2.95±0.17	4.48±0.12[b]	3.85±0.15[b,c]
Lung wet weight/dry weight	4.84±0.92	4.79±0.84	4.77±0.99
p-BNP (ng/ml)	2.19±0.011	2.33±0.034	2.31±0.031

Table 1. Effect of L-2286 treatment on gravimetric parameters and on plasma BNP in SHR. WKY: normotensive age-matched control rats, n=7, SHR-C: SHR age-matched control rats, n=8, SHR-L: SHR treated with L-2286 for 24 weeks, n=9. BW[6w]: body weight of 6-week-old rats, BW: body weight, WV: weights of ventricles, BNP: plasma b-type natriuretic peptide. Values are means±S.E.M. [a]<0.01 (vs. WKY group), [b]<0.05 (vs. WKY group), [c]<0.05 (vs. SHR-C).

4.2.2. *L-2286 treatment did not influence the levels of plasma BNP and blood pressure*

Slightly elevated plasma BNP levels were found both in SHR-C and SHR-L groups (not significant vs. WKY group). Although plasma BNP level was a little higher in SHR-C group than in SHR-L group, this difference was also not statistically significant (Table 1). In both SHR groups, blood pressure was significantly elevated compared to the WKY group ($p<0.05$). L-2286 treatment did not decrease significantly the elevated blood pressure (Table 3).

4.2.3. *L-2286 decreased the interstitial collagen deposition in the myocardium*

Histological analysis revealed slight interstitial collagen deposition in the WKY group. Chronic high blood pressure caused significantly higher collagen deposition in SHR-C rats that was significantly diminished ($p<0.05$) in the SHR-L group (Fig. 2).
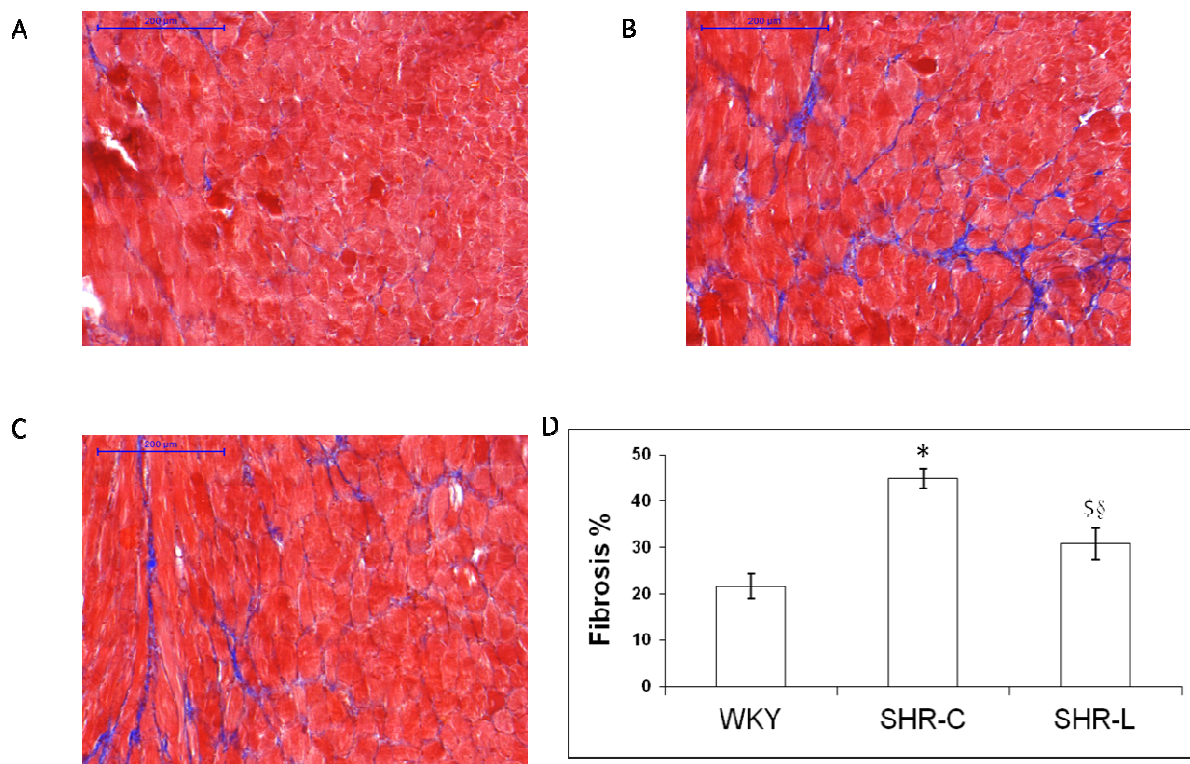
Figure 2. L-2286 treatment decreased the deposition of interstitial collagen. Sections stained with Masson's trichrome (n=5). Scale bars mean 200 µm. Magnifications 10-fold. WKY (A): normotensive age-matched control rats. SHR-C (B): 30 week-old spontaneously hypertensive rats, SHR-L (C): 30 week-old spontaneously hypertensive rats treated with L-2286 for 24 week. D: Denzitometric evaluation of the sections is shown. [*]$p<0.01$ vs. WKY, [§]$p<0.05$ vs. WKY, [$]$p<0.05$ vs. SHR-C.

4.2.4. *PARP inhibition decreased the left ventricular hypertrophy in spontaneously hypertensive rats*

At the beginning of the study the echocardiographic parameters of the three groups did not differ significantly from each other (Table 2). At the age of 30 weeks there was no significant difference in LV systolic functions (EF and FS) between the WKY and SHR groups. Heart rate did not differ significantly during the anesthesia among the groups. LVESV and LVEDV were increased significantly in SHRs (p<0.05 WKY vs. SHR-C and SHR-L), and these unfavorable alterations were not reduced by L-2286 treatment. The thickness of the septum, and the posterior wall and the relative wall thickness were also increased in SHR groups (indicating the presence of ventricular hypertrophy) comparing to the WKY group (p<0.05), and these parameters could be significantly reduced by the administration of L-2286 (p<0.05 SHR-C vs. SHR-L group) (Table 3).

	WKY	**SHR-C**	**SHR-L**
EF (%)^{6w}	67.26±0.525	68.4±1.77	68.23±1.81
FS^{6w}	38.63±4.47	38.03±5.52	39.35±4.15
LVEDV^{6w} (ml)	147.27±13.88	149.56±16.78	149.11±14.43
LVESV^{6w} (ml)	46.63±4.47	48.03±5.52	47.35±5.45
Septum^{6w} (mm)	1.2±0.07	1.18±0.05	1.17±0.12
PW^{6w} (mm)	1.19±0.07	1.16±0.067	1.14±0.04
LV mass^{6w} (uncorrected) (mg)	**344.14±35.49**	**351.66±36.23**	**354.77±33.23**

Table 2. L-2286 treatment moderately influenced the echocardiographic parameters in 6 weeks old SHRs. WKY: normotensive age-matched control rats, n=7, SHR-C: SHR age-matched control rats, n=8, SHR-L: n=9, SHR treated with L-2286 for 24 weeks.EF^{6w}: ejection fraction, FS^{6w}: fractional shortening, LVEDV^{6w}: left ventricular (LV) end-diastolic volume, LVESV^{6w}: LV end-systolic volume, Septum^{6w}: thickness of septum, PW^{6w}: thickness of posterior wall, LV mass^{6w}: weights of LVs.

	WKY	SHR-C	SHR-L
SAP[30w], (mmHg)	129±7	192±9[a]	186±5[a]
DAP[30w], (mmHg)	89±5	127±8[a]	125±4[a]
MAP[30w], (mmHg)	103±7	149±5[a]	146±7[a]
EF (%)[30w]	69.1±2.4	68.72±2.1	69.01±3.2
FS[30w]	39.8±1.9	39.04±1.85	40.57±2.66
LVEDV[30w] (ml)	279.18±18.18	335.87±10.36[a]	326.94±9.18[a]
LVESV[30w] (ml)	85.77±8.56	96.85±10.36[a]	99.81±11.85[a]
Septum[30w] (mm)	1.43±0.04	1.93±0.04[a]	1.79±0.05[a,b]
PW[30w] (mm)	1.54±0.08	2.15±0.12[a]	1.87±0.03[a,b]
RWT[30w]	0.38±0.05	0.504±0.02[a]	0.445±0.012[a,b]
LV mass[30w] (uncorrected) (mg)	1002.81±59.5	1370.35±79.87[a]	1121.13±53.23[a,b]
LV mass[30]/**BW**[30] (mg/g)	2.73±0.7	4.23±0.8[a]	3.70±0.3[a,b]

Table 3. L-2286 treatment moderately decreased the echocardiographic signs of LVHT in 30 week old SHRs. WKY: normotensive age-matched control rats, n=7, SHR-C: SHR age-matched control rats, n=8, SHR-L: n=9, SHR treated with L-2286 for 24 weeks.EF[30w]: ejection fraction, F[30w]: fractional shortening, LVEDV[30w]: left ventricular (LV) end-diastolic volume, LVESV[30w]: LV end-systolic volume, Septum[30w]: thickness of septum, PW[30w]: thickness of posterior wall, RWT[30w]: relative wall thickness, LV mass[30w]: weights of LVs. SAP, DAP, MAP[30w]: systolic, diastolic and mean arterial blood pressure at 30-week-old age (n=3 from each group). Values are mean±S.E.M. [a]p<0.05 (vs. WKY group), [b]p<0.05 (vs. SHR-C group), [c]<0.05 (vs. SHR-C).

4.2.5. Effect of L-2286 treatment on poly-ADP-ribosylation as well as on the phosphorylation state of Akt-1^{Ser473}/GSK-3β^{Ser9} and FKHR^{Ser256}

Akt-1^{Ser473} was moderately phosphorylated in WKY group. In SHR-C group, the phosphorylation of Akt-1^{Ser473} was more pronounced (p<0.01 vs. WKY). Moreover, in SHR-L rats the L-2286 treatment caused further elevation in Akt-1^{Ser473} phosphorylation (p<0.01 vs. WKY and SHR-C groups) (Fig. 3). The same result was obtained in the case of GSK-3β^{Ser9} phosphorylation (Fig. 3).
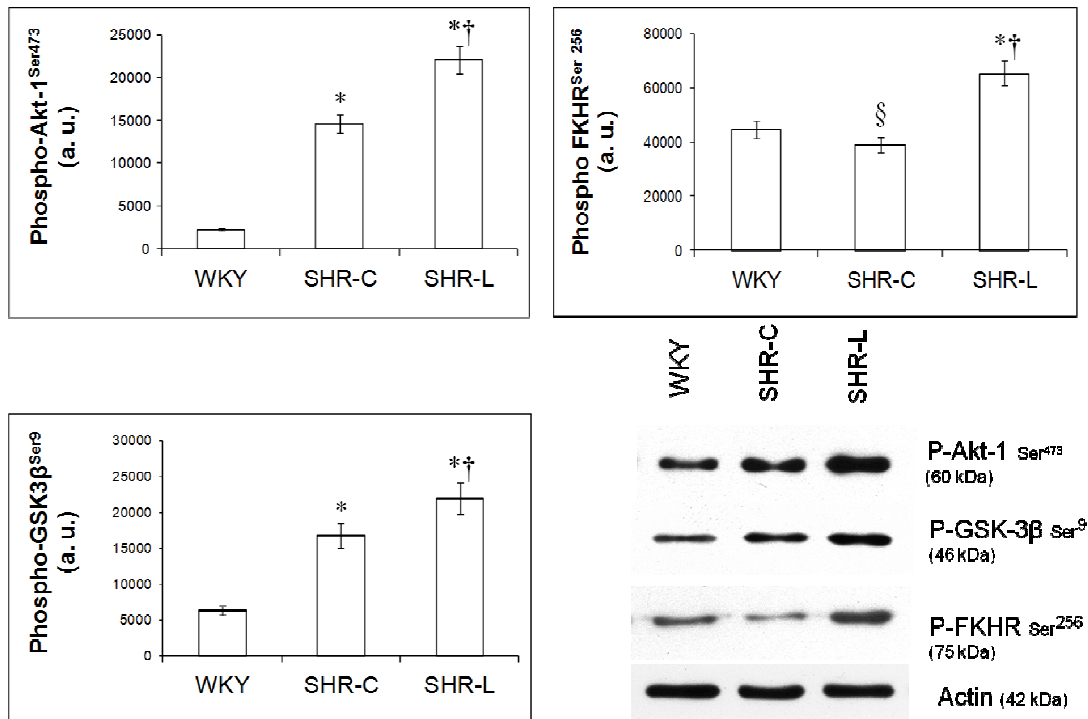
Figure 3. Effect of L-2286 treatment on Akt-1^{Ser473}/GSK-3β^{Ser9}, FKHR^{Ser256} pathway. Representative Western blot analysis of Akt-1^{Ser473}, GSK-3β^{Ser9}, FKHR^{Ser256} phosphorylation and densitometric evaluation is shown (n=4). Actin was used as loading control. Values are means±S.E.M. WKY: normotensive age-matched control rats. SHR-C: 30 week-old spontaneously hypertensive rats, SHR-L: 30 week-old spontaneously hypertensive rats treated with L-2286 for 24 weeks. *p<0.01 vs. WKY, †p<0.01 vs. SHR-C, §p<0.05 vs. WKY.

To detect the effectivity of L-2286, the ADP-ribosylation of the samples were analysed by Western-blot. The lowest degree of ADP-ribosylation was present in SHR-L group, and the most pronounced ADP-ribosylation was seen in SHR-C group (p<0.05 vs. WKY) (Fig. 4). Another target protein of Akt-1^{Ser473} (besides GSK3β^{Ser9}) is FKHR^{Ser256}. Consistently with the result of Akt-1^{Ser473} phosphorylation, the strongest phosphorylation (therefore inhibition) could be observed in SHR-L group (p<0.01 vs. SHR-C and WKY). The lowest phosphorylation and therefore the highest activity of FKHR was seen in SHR-C group (p<0.05 vs. WKY, Fig. 3).

4.2.6. Effect of L-2286 on the amount of Hsp72 and 90

There was no significant difference among the three groups in the level of Hsp72. On the other hand, the level of Hsp90 was elevated in SHR-L group compared to WKY and

SHR-C groups (p<0.01 SHR-L vs. WKY or SHR-C groups), and the lowest amount of this protein was present in WKY samples (Fig. 4).
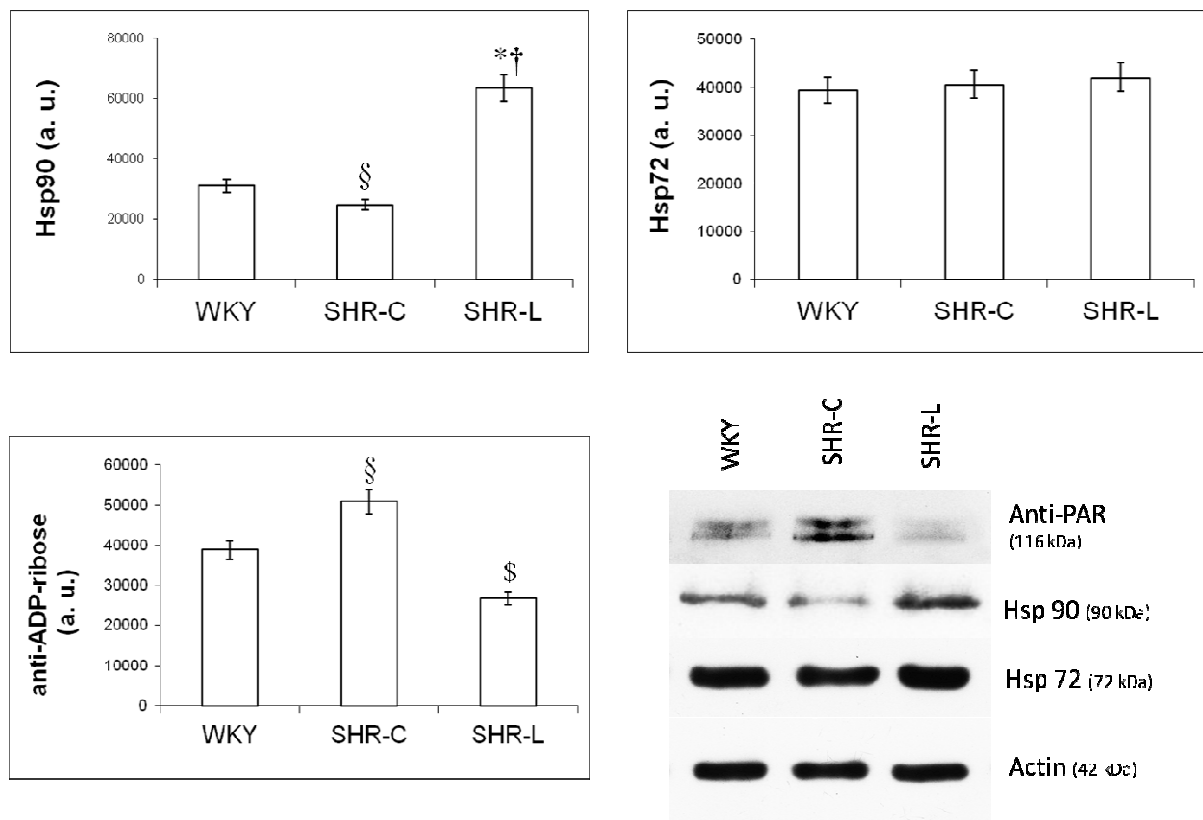

Figure 4. Effect of L-2286 treatment on the level of Hsp72, 90 and poly(ADP-ribos)ylation. Representative Western-blot analysis of Hsp72, 90, anti-PAR and densitometric evaluations are shown (n=4). Actin was used as loading control. Values are means±S.E.M. WKY: normotensive age-matched control rats. SHR-C: 30 week-old spontaneously hypertensive rats, SHR-L: 30 week-old spontaneously hypertensive rats treated with L-2286 for 24 weeks. *p<0.01 vs. WKY, †p<0.01 v.s SHR-C, §p<0.05 vs. WKY, $p<0.05 vs. SHR-C

4.2.7. *Effect of L-2286 administration on MAPKs*

Phosphorylation of p38-MAPK$^{Thr180-Gly-Tyr182}$, ERK 1/2$^{Thr183-Tyr185}$ and JNK was the lowest in the WKY group compared to SHR-C and SHR-L groups (p38-MAPK$^{Thr180-Gly-Tyr182}$: p<0.01 vs. SHR groups, ERK 1/2: p<0.05 vs. SHR groups, JNK: p<0.05 vs. SHR groups). In the case of p38-MAPK$^{Thr180-Gly-Tyr182}$ and JNK, their phosphorylation was elevated in both SHR-C and SHR-L groups, but there were no significant differences between the two SHR groups (Fig. 5, JNK: data not shown).

Phosphorylation of ERK $1/2^{Thr183-Tyr185}$ was increased significantly in SHR-C and SHR-L groups. L-2286 treatment did not alter significantly the phosphorylation in SHR-L group compared to the SHR-C group (Fig. 5).
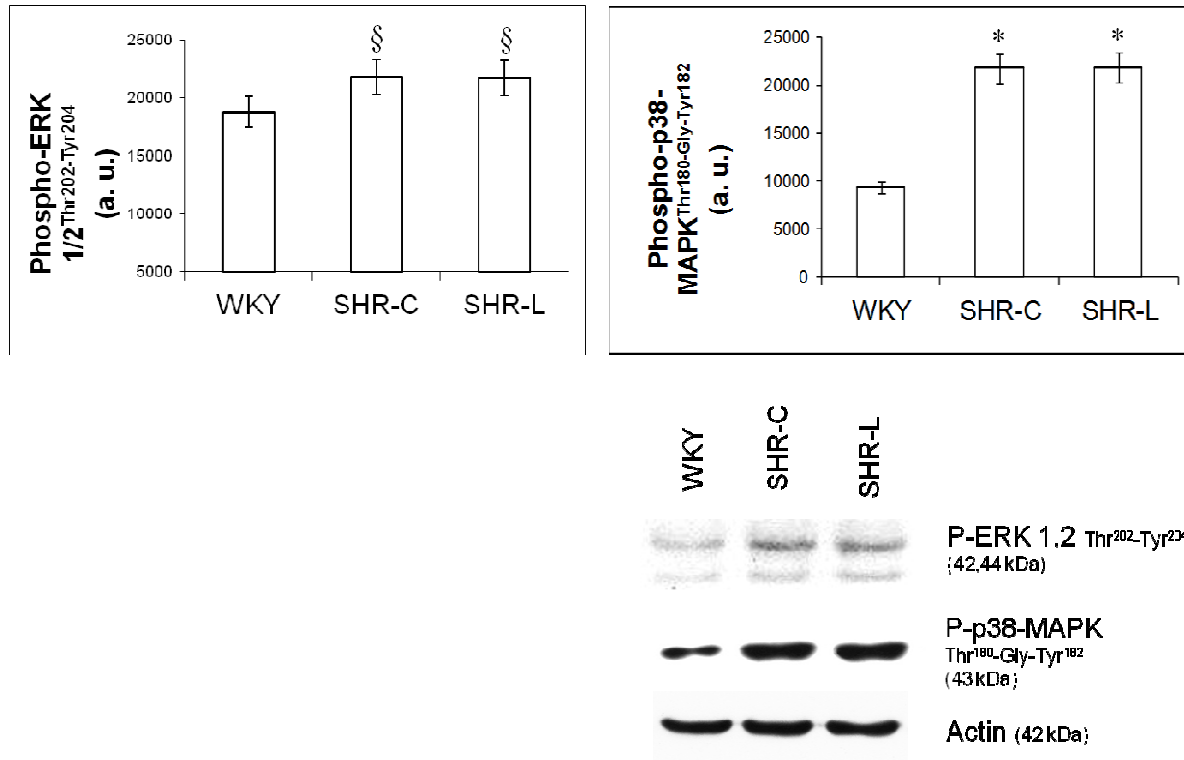

Figure 5. Effect of L-2286 on the phosphorylation state of MAPK pathway. Representative Western blot analysis of ERK $1/2^{Thr183-Tyr185}$, and p38-MAPK$^{Thr180-Gly-Tyr182}$ phosphorylation and densitometric evaluation is shown (n=4). Actin was used as loading control. Values are means±S.E.M. WKY: normotensive age-matched control rats. SHR-C: 30 week-old spontaneously hypertensive rats, SHR-L: 30 week-old spontaneously hypertensive rats treated with L-2286 for 24 weeks. $^{§}p<0.05$ vs. WKY $^{*}p<0.01$ vs. WKY.

4.2.8. *Influence of L-2286 treatment on the phosphorylation state of several PKC isoforms*

The overall (pan) phosphorylation of PKC (pan βII^{Ser660}) was low in the WKY group and became significantly higher in SHR-C and SHR-L groups ($p<0.01$ WKY vs. SHR groups). Administration of L-2286 could not affect the phosphorylation state of PKC pan βII Ser^{660} in SHR-L group compared to the SHR-C group (Fig. 6).
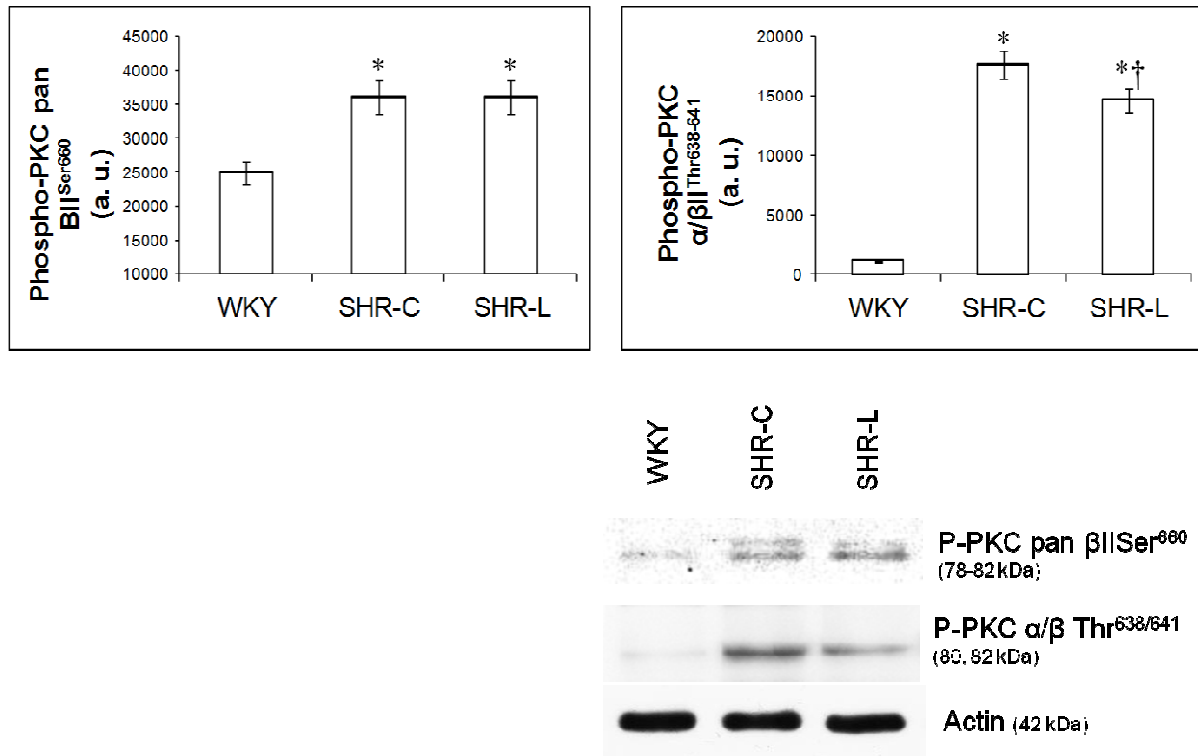
Figure 6. Effect of L-2286 administration on the activity of PKC isoenzymes. Representative Western blot analysis of PKC pan βII^{Ser660} and PKC $\alpha/\beta II^{Thr638/641}$ phosphorylation and densitometric evaluations are shown (n=4). Values are means±S.E.M. WKY: normotensive age-matched control rats. SHR-C: 30 week-old spontaneously hypertensive rats, SHR-L: 30 week-old spontaneously hypertensive rats treated with L-2286 for 24 weeks. [*]p<0.01 vs. WKY, [†]p<0.01 vs. SHR-C.

The lowest phosphorylation could be observed in the WKY group in case of PKC $\alpha/\beta II^{Thr638/641}$, δ^{Thr505}, $\zeta/\lambda^{Thr410/403}$ and ϵ^{Ser729} (p<0.01 vs. SHR groups). As PKC ζ antibody, we used a combined antibody (i.e. PKC ζ/λ $Thr^{410/403}$), which did not discriminate between PKC ζ and λ; PKC λ being structurally highly homologous to PKC ζ in the COOH-terminal end of the molecule (62). L-2286 treatment decreased significantly the phosphorylation of PKC $\alpha/\beta II$ $^{Thr638/641}$ and ζ, while it could increase the phosphorylation of ϵ^{Ser729} (PKC $\alpha/\beta II$ $^{Thr638/641}$, ζ, ϵ^{Ser729}: p<0.01, SHR-L vs. SHR-C) (Fig. 6,7). In the case of PKC δ^{Thr505} there was no significant difference between the SHR groups (Fig. 7).
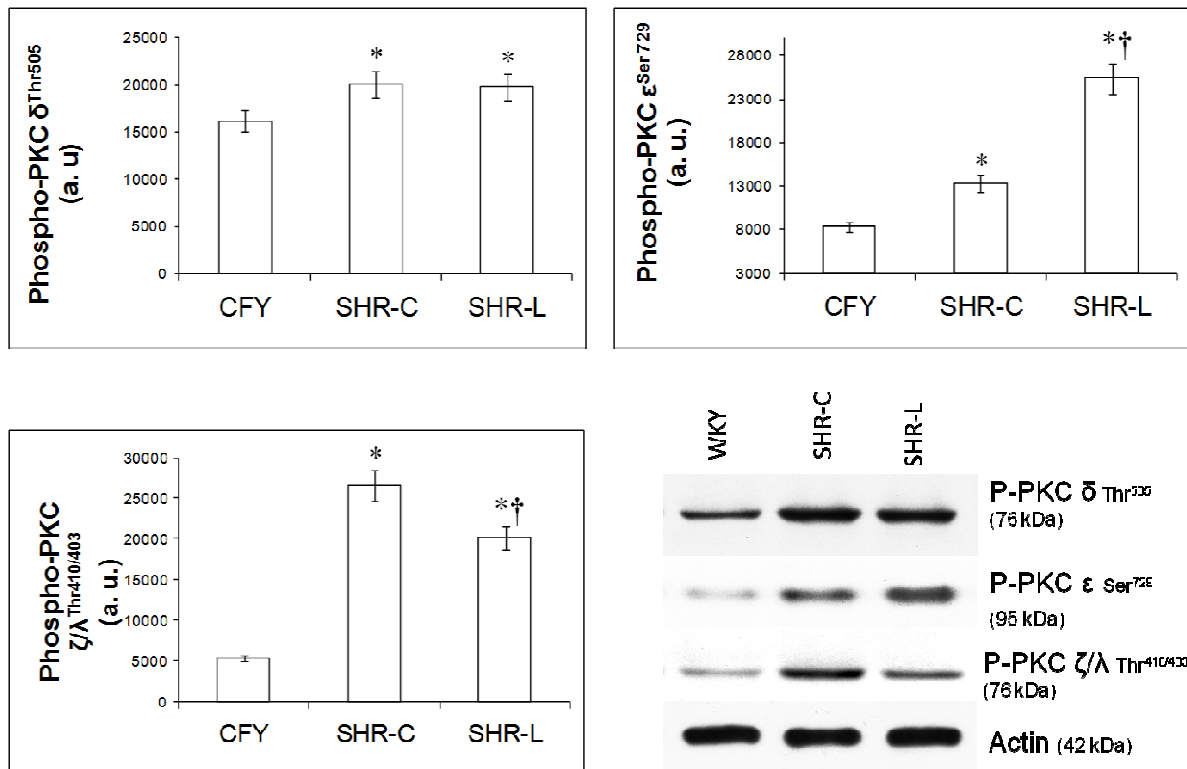
Figure 7. Effect of L-2286 administration of PKC isoenzymes. Representative Western blot analysis of PKC δ^{Thr505}, ε^{Ser729} and $\zeta/\lambda^{Thr410/403}$ phosphorylation and densitometric evaluation is shown (n=4). Actin was used as loading control. Values are means±S.E.M. WKY: normotensive age-matched control rats. SHR-C: 30 week-old spontaneously hypertensive rats, SHR-L: 30 week-old spontaneously hypertensive rats treated with L-2286 for 24 weeks. *p<0.01 vs. WKY, †p<0.01 vs. SHR-C.

4.3. Discussion

The major findings of this study are that chronic inhibition of nuclear PARP enzyme reduces the excessive ADP-ribosylation of nuclear proteins, beneficially influences the intracellular signaling pathways and thus prevents the development of cardiac hypertrophy, which is an early consequence of hypertension. We used the SHR model that is considered to be a relevant animal model for essential hypertension in humans (42). Our study began at a very early age (6-week-old) of SHRs, because at this age the blood pressure of animals is still normal and the hearts show no signs of remodeling. However, by the end of the study (30 weeks), the signs of marked hypertensive cardiopathy develop in SHRs. Effect of L-2286 on wild type WKY rats was also examined, but it was inconclusive on the intact hearts (data not shown) as it was expected. Therefore, data of L-2286 treated WKY rats are not shown.

Previously, we have proved that PARP-inhibition could inhibit the transition of hypertensive cardiopathy to end-stage heart failure (32), but there is no data about the role of PAPR-inhibitors against the development of early consequences of hypertension.

Hypertension is a major risk factor for cardiovascular mortality and morbidity, and it is associated with left ventricular hypertrophy and diastolic dysfunction and later with systolic dysfunction and it can lead to heart failure. There is a strong correlation between left ventricular mass and the development of cardiovascular pathogies (43). The development of long-term hypertension-induced myocardial remodeling can be explained by different mechanism in the literature, but oxidative stress and abnormal signaling are generally respected as the molecular basis of the disease. Peroxynitrite and other reactive species induce oxidative DNA damage and consequent activation of the nuclear enzyme PARP. In related animal models of disease, pharmacological inhibition of PARP provides significant therapeutic benefits (44).

4.3.1. PARP inhibition and gravimetric parameters in SHR

Significant LV hypertrophy develops by the age of 3 months in SHR animals but it is more often studied closer to 6 months of age (45). In our SHR rats myocardial hypertrophy developed, as increased WV/BW ratio could be observed. We could not observe any obvious signs of HF, because BNP activity and the index of pulmonary congestion was not elevated compared to the WKY group.

4.3.2. *PARP inhibition and interstitial collagen deposition in SHR*

Chronic hypertension leads to excessive collagen deposition (fibrosis) as part of the process of cardiovascular remodeling. In our previous studies, when SHR or postinfarcted animals exhibited overt heart failure, L-2286 also prevented interstitial fibrosis and adverse structural remodeling (31, 32). In the present study, our results suggest that PARP inhibitor treatment can exert marked antifibrotic effect already in this early stage of hypertensive heart disease.

4.3.3. *PARP inhibition and echocardiographic parameters*

In our experiment the systolic LV function was not decreased in SHR rats during the 24-week-long treatment. It is in accordance with several other studies (34, 35, 36) involving different experimental models of pressure overload-induced hypertrophy. During the development of hypertension, alterations in LV geometry may also occur as an adaptation to increased pressure overload. In hypertensive patients, LV geometry can be classified into four patterns on the basis of LV mass index and RWT and these patterns have been shown to be closely related to LV function and to patients' prognosis. In this study, increased RWT and increased WV/BW were found, which indicates concentric LV hypertrophy (35). L-2286 treatment decreased significantly the signs of left ventricular hypertrophy (wall thickness and RWT) even though the elevated blood pressure of SHR rats was not influenced by PARP inhibition.

4.3.4. *L-2286 treatment and the activity of Akt-1^{Ser473}/GSK3β^{Ser9} and FKHR^{Ser256} pathway*

Previous works demonstrated that PARP inhibitors can induce the phosphorylation and activation of Akt-1 in reperfused myocardium, thus raising the possibility that the protective effect of PARP inhibition can be mediated through the activation of the prosurvival phosphatidylinositol-3-kinase (PI3-kinase)/Akt-1 pathway (46). Akt-1 is a key molecule in the signaling cascade of physiological hypertrophy (47). Recent results demonstrate an important role of Akt/m-TOR signaling in cardiac angiogenesis, whose disruption contributes to the transition from hypertrophy to HF (14). In our experiment, the phosphorylation of Akt-1^{Ser473} was far the lowest in WKY group and the highest in SHR-L group. Phosphorylation

and therefore the inhibition of GSK-3β^{Ser9} and Foxo1 (FKHR) (downstream targets of Akt-1) (48, 49) were also determined. This showed the same pattern as the phosphorylation of Akt-1. The similar results were obtained in our studies using PARP inhibitors (16,46) or by suppressing PARP-1 activation by siRNA technique (15). These results may indicate that SHR-C animals tried to compensate for the adverse effects of chronic hypertension, but failed to do so. On the other hand, L-2286 treatment further elevated Akt activation that could, at least partially, account for the beneficial changes in the cardial remodeling of the SHR-L animals.

4.3.5. L-2286 administration and levels of Hsp 72 and 90

Cellular stress leads to the expression of Hsp's (50). They are known to protect the myocardium from the damaging effects of ischemia and reperfusion (51). According to the results of Jiang et al. (51) and Shinohara et al. (52) the Hsp's can preserve the mitochondrial respiratory function and structure which are damaged in case of cell death. The flux of pro-apoptotic proteins can be induced by various stimuli, one of them is the decreased level of ATP. This can be induced by overactivation of PARP-1, which consumes too much ATP in certain pathologic conditions (53). In case of Hsp90 in our study, the level of it was increased by long-term L-2286 treatment. Besides the activation of Akt-1^{Ser473}, this can contribute to the cell survival in L-2286 treated rats. The level of Hsp72 was not influenced significantly by L-2286 administration in our investigation.

4.3.6. L-2286 administration and MAPKs in young SHR

Previous works demonstrated that PARP inhibitors have a moderate effect on MAPKs in acute phase of myocardial infarction and in postinfarction heart failure (31, 46). MAPKs are ubiquitously expressed and their activation is observed in different heart diseases, including hypertrophic cardiomyopathy, dilated cardiomyopathy, and ischemic/reperfusion injury in human and animal models (54). In our study, the phosphorylation of p38-MAPK$^{Thr180-Gly-Tyr182}$, JNK and ERK 1/2$^{Thr183-Tyr185}$ was elevated both in SHR-C and SHR-L groups. Our results are consistent with the results of Kacimi et Gerdes (55) using

spontaneously hypertensive heart failure (SHHF) rats. L-2286 treatment did not influence the phosphorylation of p38-MAPK and JNK. The role of JNK and p38-MAPK-signaling in cardiac hypertrophy is not fully clarified (14). In the myocardium, both p38-MAPK and JNK transduction cascades have been implicated in regulating the hypertrophic response as well as cardiomyopathy and HF (56). The result of JNK is consistent with our result of Hsp72, because the level of the latter was not altered by L-2286, and it was demonstrated that Hsp72 downregulates JNK by accelerating its dephosphorylation (52).

The elevated blood pressure may have induced ERK activation (12). Accordingly, activation of ERK1/2 was the lowest in WKY group, and was higher in SHR-C. Phosphorylation of ERK1/2 was not elevated by L-2286 administration in this study. The in vivo role of ERK in cardiac hypertrophy has been demonstrated in several genetically engineered animal models. Cardiac-specific expression of constitutively activated MEK1 promotes cardiac hypertrophy without compromised function or long-term animal survival, suggesting that activation of ERK activity promotes a compensated form of hypertrophy (54). All these results suggest that MAPK activation did not participate significantly in mediating the adverse cardiac effects of chronic hypertension in our model.

4.3.7. PARP inhibition and PKC pathways in young SHR

PARP inhibitors were found to affect PKC isoenzymes (31, 46). The levels of all PKC isoforms increased in SHR groups compared to the WKY group in our study. Our results are in agreement with Koide et al. (13) using Dahl Salt-Sensitive rats in cardiac hypertrophy stage. Recent studies suggested that PKC is critically involved in the development of cardiac remodeling and HF. The data also suggest that individual PKC isoforms have different effects on cell signaling pathways, variously leading to changes in cardiac contractility, hypertrophic response and tolerance to myocardial ischaemia in the heart (13).

Activation of PKC pan βII^{Ser660} and δ^{Thr505} were not altered by L-2286 treatment, while activation of $\alpha/\beta II^{Thr638/641}$ and $\zeta/\lambda^{\ Thr410/403}$ were attenuated and activation of ϵ^{Ser729} was augmented by L-2286. These alterations can mediate – at least partly – the favourable cardiovascular effects of L-2286, similarly as it was found in previous works (31, 46).

PKC α is the most extensively expressed among the myocardial PKC isoforms, and it is a key regulator of cardiomyocyte hypertrophic growth (57, 58). PKC α was sufficient to stimulate

cell hypertrophy (59). Transgenic mice overexpressing PKC β2 exhibited cardiac hypertrophy and decreased LV performance; this depressed cardiac function improved after the administration of a PKC β-selective inhibitor (60). Previous reports suggest that PKC α and β and PKC ζ/λ are involved in the development of cardiac hypertrophy and HF. Additionally, PKC ε plays a role in physiological hypertrophic responses (13, 61), has cardioprotective effect (62) and by interacting with Akt-1 and affecting Bcl-2 promote vascular cytoprotection (63). Accordingly, in our study, both the activity of Akt-1^{Ser473} and PKCε^{Ser729} were elevated by L-2286 administration.
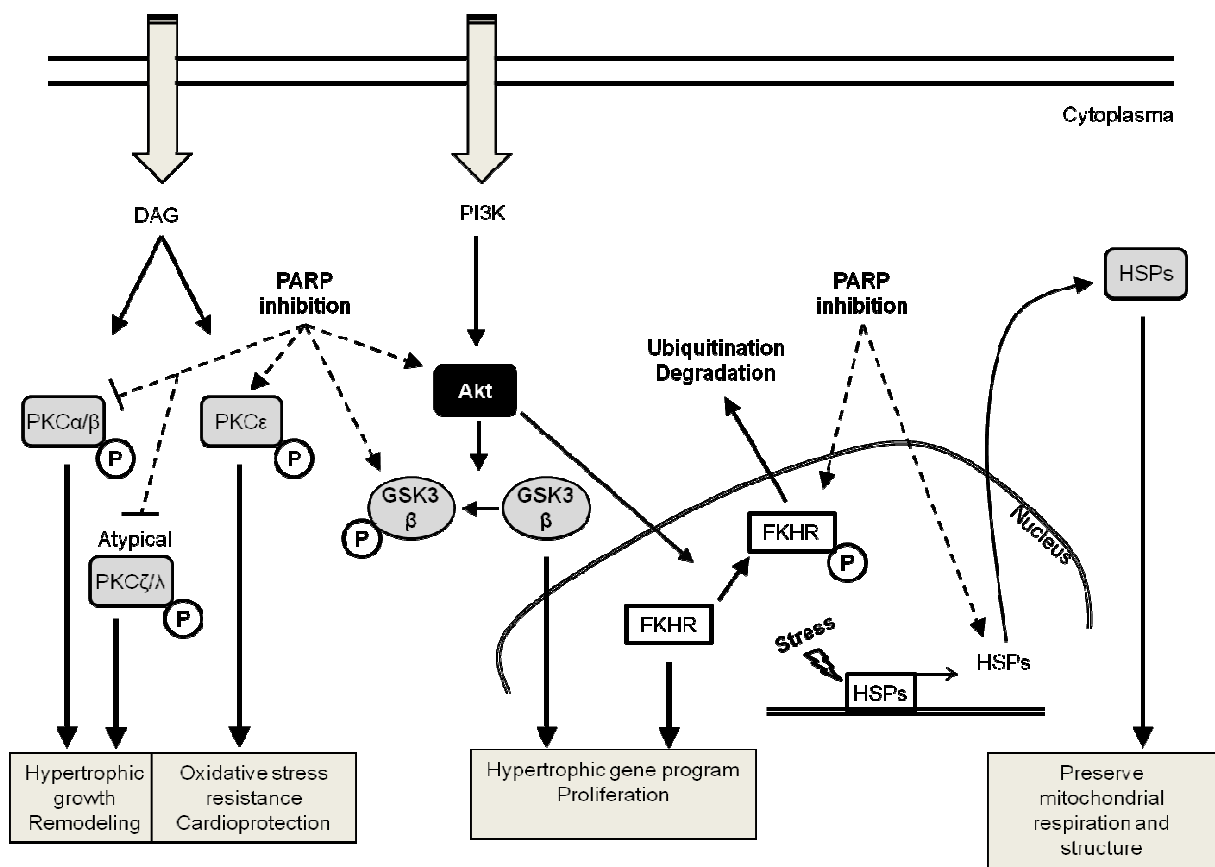

Figure 8. Summary of pathway alterations due to L-2286 treatment.

5. EFFECTS OF BRADYKININ B1 RECEPTOR ANTAGONISM IN HYPERTENSIVE ORGAN DAMAGES

5.1. Materials and methods

5.1.1. Ethics Statement

The investigation conforms to the Guide for the Care and Use of Laboratory Animals published by the U.S. National Insitutes of Health (NIH Publication No. 85-23, revised 1996), and was approved by the Animal Research Review Committee of the University of Pecs, Medical School.

5.1.2. Animals and treatment groups

Animals: 45 male spontaneously hypertensive rats (SHR) (Charles River Laboratories, Budapest, Hungary). The animals were approximately 8 weeks old on arrival and weighed approximately 250-270 g.

Body weight, food consumption measurements were performed weekly (on every Monday) during the test period (except of age matched WKY group). Echocardiography measurements were performed during Weeks 0 and 26, blood pressure measurements were performed during Weeks 0, 13 and 26.

The animals were anaesthetized with a mixture of 3,5 % isoflurane (Forane) and 96,5 % oxygen and killed by heart excision on Week 26. Before kill, whole blood samples (approximately 1 ml) were obtained by cardiac puncture. Heart, great vessel and eye samples were collected during necropsy and prepared for further analyses.

Group 1: 15 animals receiving control diet (0 ppm concentration) (Control group).

Group 2: 15 animals receiving test diet mixed with FGY-1153 at 120 ppm concentration (estimated to yield a dose level of approximately 6 mg/kg/day) (FGY120 group).

Group 3: 15 animals receiving test diet mixed with FGY-1153 at 400 ppm concentration (Estimated to correspond to a dose level of approximately 20 mg/kg/day) (FGY400 group).

Group 4: 10 age-matched Wistar-Kyoto rats, receiving control diet (0 ppm concentration) (WKY group).

5.1.3. Administration of the test item

The treatment with FGY-1153 started at the age of about 11-weeks. During the whole duration of the study (26 weeks) animals were treated orally, using standard rat chow containing FGY-1153 (in 120 ppm or 400 ppm), or control rat diet. The rat chow was available to the animals *ad libitum*.

5.1.4. Investigations and measurements

Food consumption

During the last 2 weeks of the acclimatisation period, all animals received Control test diet (0 ppm concentration) for adaptation. The quantity of food consumed by each cage of animals was measured and recorded daily during the adaptation period. The quantity of food consumed by each cage of animals was measured and recorded once weekly during the treatment period (except of age-matched WKY group).

Body weight

Body weights were measured and recorded once weekly during the acclimatization and treatment periods and on the day of necropsy (except of age-matched WKY group).

Measurement of blood pressure

Non-invasive blood pressure measurements were performed on each animal at three occasions during Weeks 0, 13 and 26 of the study. Blood pressure measurements were performed by non-invasive tail-cuff method. Blood pressure was measured by Hatteras SC1000 Blood Pressure Analysis System with rat species platform (Hatteras Instruments Inc.) (except for age-matched WKY group).

5.1.5. Echocardiographic examinations

Transthoracic two dimensional echocardiography (n=7 from each groups) under inhalation anesthesia was performed at the beginning of the experiment and on the day of sacrifice. Rats were lightly anaesthetized with a mixture of 1.5% isoflurane (Forane) and 98.5% oxygen. The chests of the animals were shaved, acoustic coupling gel was applied, and warming pad was used to maintain normothermia. Rats were imaged in the left lateral decubitus position. Cardiac dimensions and functions were measured from short- and long-axis views at the mid-papillary level by a VEVO 770 high-resolution ultrasound imaging system (VisualSonics, Toronto, Canada) - equipped with a 25 MHz transducer. LV ejection fraction (EF), left ventricular (LV) end-diastolic volume (LVEDV), LV end-systolic volume (LVESV), LV inside dimensions (LVIDd and LVIDs), E/E' and the thickness of septum and posterior wall (PW) were determined. EF (%) was calculated by: 100x((LVEDV - LVESV)/LVEDV); relative wall thickness (RWT) was calculated by: (PW thickness + interventricular septal thickness)/LVIDd.

5.1.6. Investigation of vascular and cardiac remodeling with histology and immunohistochemistry

Heart, carotid arteries and aortic segments excised for histological processing were fixed immediately after excision in buffered paraformaldehyde solution (4%) for 1 day. Five µm thick sections were cut. Slices were stained with Masson's trichrome staining to detect the interstitial fibrosis.

The intima-media thickness was measured on cross sections of histological preparations from great arteries with Mirax viewer software (version: 1.12.22.0).

For assessment of cardiac fibrosis, five samples were taken from all cross-sectioned cardiac preparations at constant magnification from separate, continuous territories excluding perivascular, sub-endo- and sub-pericardial areas. Different stainings were discriminated by Colour deconvolution plugin for ImageJ with built-in colour vectors for Masson's trichrome. After autotresholding, the area fraction of aniline-blue staining was measured in each sample and ANOVA analysis was performed.

For evaluation of vascular fibrosis, five different areas (ROIs) from the territories of the tunica media layers of aorta and carotid arteries were selected, where measurements have

been made. Different stainings were discriminated by Colour deconvolution plugin for ImageJ with built-in colour vectors for Masson's trichrome. After autotresholding, the area fraction of aniline-blue staining has been measured in each predefined ROIs. On carotis data Square root transformation has been made.

Immunohistochemical staining was performed for nitrotyrosine. Primary antibody used for the staining was monoclonal mouse anti-nitrotyrosine antibody. Sections were quantified with the NIH ImageJ analyzer system.

5.1.7. *Electron microscopic evaluation of cardiac and vascular remodeling*

Electron microscopic examinations were performed on hearts and great vessels from the treated and control SHR animals. The fixative was supplemented with 1% glutaraldehyde. After washing, samples were stained with 1% OsO_4 in PB, dehydrated through ascending ethanol series and embedded in Durcupan ACM resin. Sections were cut, counterstained with Reynold's lead citrate, and examined and photographed in a JEOL 1200 EX electron microscope. All histological samples were examined by an investigator in a blinded fashion.

5.1.8. *Western blot analysis of heart and great vessels*

Heart samples, carotid arteries and aortic segments were homogenized in ice-cold 50 mM Tris-buffer, pH 8.0 (containing protease inhibitor cocktail 1:1000, and 50 mM sodium vanadate) and harvested in 2x concentrated SDS-polyacrylamide gel electrophoresis sample buffer. Proteins were separated on 10 or 12% SDS-polyacrylamide electrophoresis gel and transferred to nitrocellulose membranes. After blocking (2 h with 3% non-fat milk in Tris-buffered saline), membranes were probed overnight at 4°C with antibodies recognizing the following antigens: anti-N-terminal domain of actin (1:10,000), TGF-beta (1:1000), phospho-specific SMAD2 $Ser^{465/467}$(1:1000), phospho-specific Akt Ser^{473} (1:1000), phospho-specific GSK-3-beta Ser^9 (1:1000). Membranes were washed six times for 5 min in Tris-buffered saline (pH 7.5) containing 0.2% Tween (TBST) before addition of goat anti-rabbit horseradish peroxidase-conjugated secondary antibody (1:3000 dilution). The antibody–antigen

complexes were visualized by means of enhanced chemiluminescence. After scanning, results were quantified by NIH Image J program.

5.1.9. Blood sampling

To assess drug plasma exposures, blood samples were collected from the rats by direct cardiac puncture on the last day of the study just before necropsy between 08.20 am and 12.20 pm. The blood samples were drawn into either heparinized tubes or Lavender Vacutainer tubes containing EDTA. Taking some of the samples into EDTA containing tubes instead of heparinized tubes was a deviation from protocol by mistake. However, by applying corresponding calibration method this technical difference was considered not to affect accuracy of the measurement. The blood samples were centrifuged at 1600 *g* for 15 min at 4°C to separate plasma. Supernatants were collected and kept at −70°C.

5.1.10. Statistical analysis

All data are expressed as mean ± SEM. For comparison of WKY and Control groups, independent sample's t-test (2-tailed) was applied. Control and Treatment groups were analyzed using one-way ANOVA (SPSS for Windows 20.0). For *post hoc* comparison Dunnett's test (2-tailed) was chosen. In cases of inhomogeneous group variances Welch correction was applied followed by Dunnett T3 *post hoc* test. Values of $p < 0.05$ were considered statistically significant.

5.2. Results

5.2.1. Effect of FGY-1153 on body weight

Body weights were measured and recorded once weekly during the treatment period. There were no significant differences between the three groups (Fig. 9).
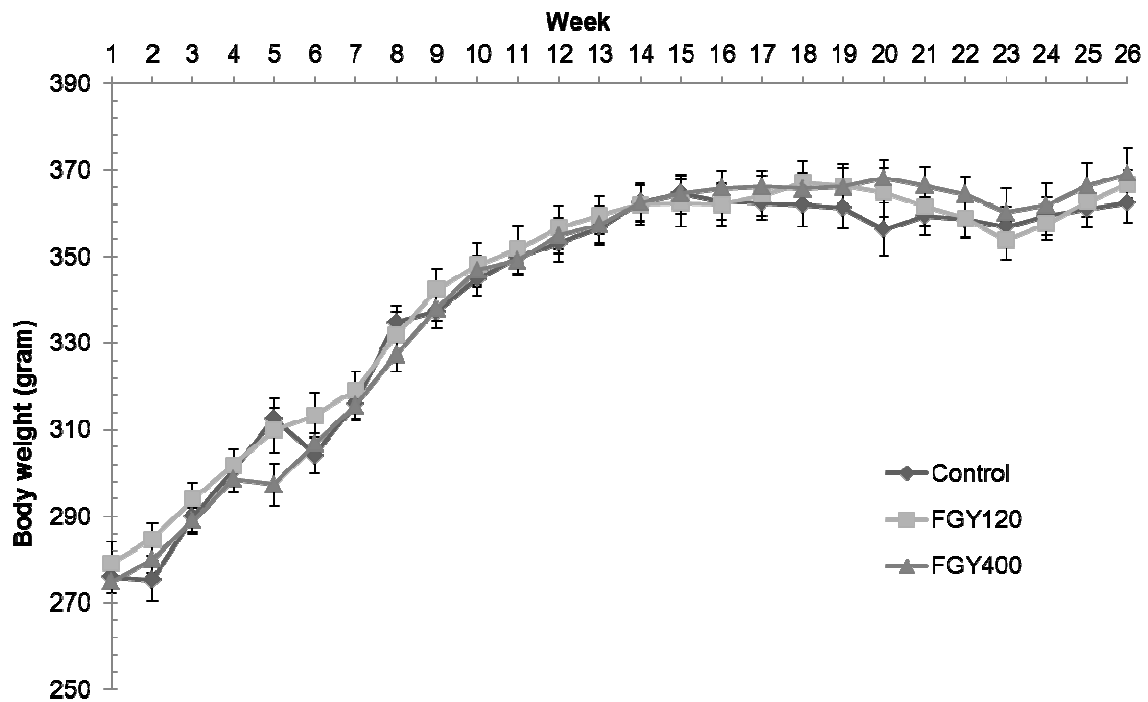

Fig. 9. Effect of FGY-1153 on body weight during the treatment period. Data are presented as mean±S.E.M. One-way ANOVA analysis conducted for each week did not reveal statistically significant differences between groups.

5.2.2. Effect of FGY-1153 on food consumption

The quantity of food consumed by each cage of animals was measured and recorded once weekly during the treatment period. There were no overt differences between the food consumptions of the three groups throughout the study. (Fig. 10).
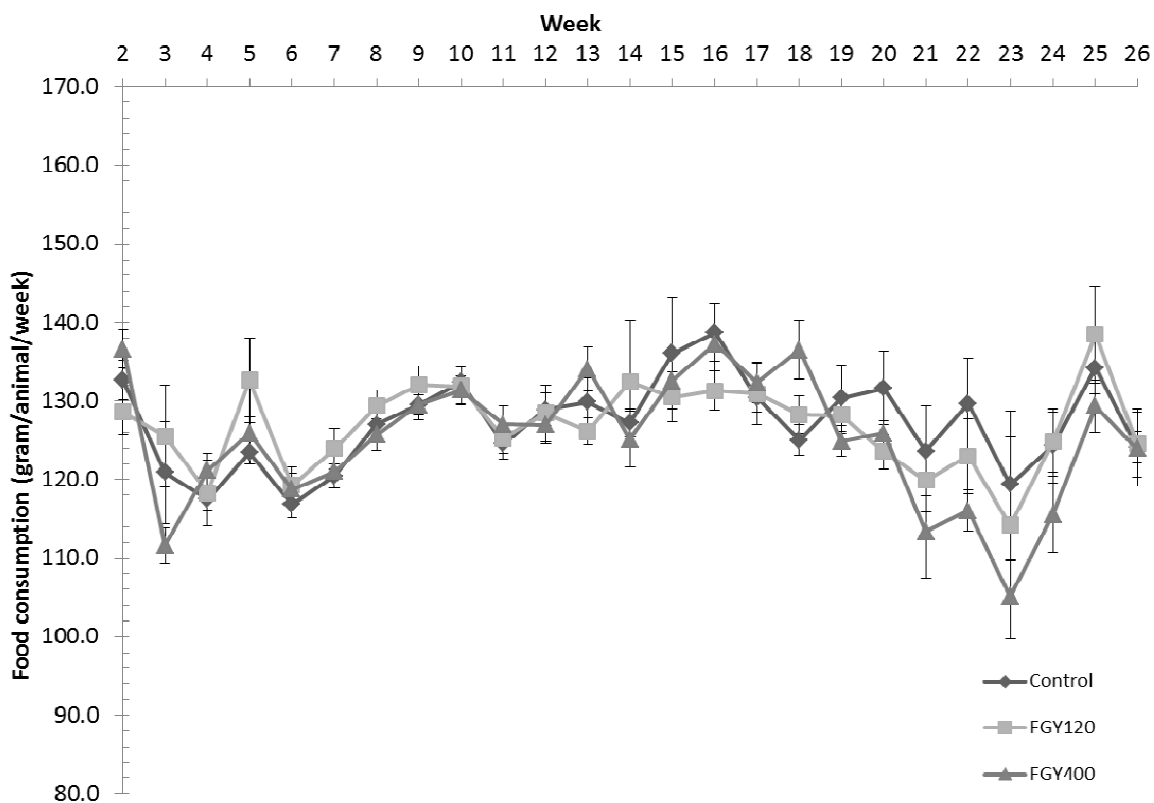
Fig. 10. Effect of FGY-1153 on food consumption during the treatment period. Data are presented as mean±S.E.M. Data were analysed with one-way ANOVA. No statistically significant differences were found at any time points between the groups.

5.2.3. Dose calculation of FGY-1153

The weekly calculated dose of test substance was 6.32 ± 0.14 (ranged from 5.51 ± 0.47 to 7.76 ± 0.14) mg/kg/day in the FGY120 group and 20.9 ± 0.59 (ranged from 16.6 ± 0.4 to 28.0 ± 0.3) mg/kg/day in the FGY400 group.

5.2.4. Effect of FGY-1153 on blood pressure

At the beginning of the study there was no significant difference between the mean arterial blood pressure of the three groups (Control: 178.71±3.488 mm Hg, FGY120 group: 172.47±3.810 mm Hg, FGY400 group: 174.53±2.303 mm Hg, p=0.374). The FGY-1153 treatment seemed to have no significant effect on blood pressure parameters either at Week 13 or Week 26. Mean arterial blood pressure values did not differ significantly between the groups at Week 13 (Control: 215.93±6.114 mm Hg, FGY120 group: 212.73±5.682 mm Hg,

FGY400 group: 228.80±4.488 mm Hg, p=0.096) and at Week 26 (Control: 256.36±8.039 mm Hg, FGY120 group: 256.80±7.693 mm Hg, FGY400 group: 275.33±3.067 mm Hg, p=0.078).

Nevertheless, a non-significant trend of higher blood pressure in the FGY400 group compared to the other two groups was apparent.

5.2.5. *Effect of FGY-1153 on echocardiographic parameters*

Compared to the parameters measured at the beginning of the study, the septum and posterior wall thicknesses increased in all groups during the treatment period. However treatment with both low dose and high dose FGY-1153 significantly attenuated the elevation of these parameters indicating that the treatment with FGY-1153 reduced the hypertension induced left ventricular hypertrophy.

LVIDs and LVESV were also increased in all groups during the study, the elevation of these parameters were however significantly attenuated in the FGY120 group, but not in the FGY400 group. Left ventricular systolic function - expressed as ejection fraction (EF%) - showed a decreasing tendency in both the Control group and the FGY400 group by the end of the study compared to the initial parameters. In comparison with the Control group these changes were however significantly attenuated in the FGY120 group, indicating that the low dose FGY-1153 treatment prevented the hypertension induced decrease in systolic left ventricular function. The E/E' ratio showed an increasing tendency during the study in the Control group, while this parameter was significantly decreased in both of the FGY120 and FGY400 groups. It may indicate that FGY-1153 treatment could attenuate the diastolic dysfunction seen in SHR rats.

In the last column of Table 5 the typical values of structural and functional parameters of age-matched normotensive animals (WKY group) can be seen.

	SHR Week 0	Control Week 26	FGY120 Week 26	FGY400 Week 26	WKY age-matched
Septum (mm)	1.66 ± 0.01	2.09 ± 0.04	1.90 ± 0.04**	1.88 ± 0.02**	1.67 ± 0.07**
Post. Wall(mm)	1.58 ± 0.02	1.94 ± 0.02	1.82 ± 0.01*	1.81 ± 0.04*	1.644 ± 0.11*
LVIDd	7.28 ± 0.07	8.28 ± 0.08	7.94±0.09*	7.98 ± 0.11	8.00 ± 0.25
LVIDs	4.40 ± 0.07	5.38 ± 0.09	4.85 ± 0.08**	5.12 ± 0.14	4.52 ± 0.12**
LVEDV (ml)	280.49 ± 6.06	373.54 ± 8.11	340.79 ± 9.25*	344.72 ± 10.78	349.85± 24.66
LVESV (ml)	88.72 ± 3.33	141.56 ± 5.89	111.69 ± 4.15**	127.31 ± 8.66	97.07 ± 5.54**
EF (%)	68.48 ± 0.75	62.16 ± 1.24	67.10 ± 1.33*	63.36 ± 1.37	71.67 ± 0.87**
E/E'	35.16 ± 1.54	42.17 ± 5.26	30.05 ± 0.86*	26.50 ± 2.77*	30.00 ± 2.26
RWT	0.447 ± 0.004	0.485 ± 0.014	0.469 ± 0.007	0.464 ± 0.011	0.413 ± 0.01**

Table 5. Evaluation of echocardiographic parameters. Data of all animals are presented in the first column (SHR Week 0, N=21) at the beginning of the study and data from the three groups (Control, FGY120, FGY400 Week 26) (N=7 in each groups) are indicated at the end of the treatment period. Last column represents the data of age-matched normotensive animals (WKY, N=7). Values are expressed as mean±S.E.M. Comparisons between WKY and Control groups were made by independent samples t-test. Data of Control and Treatment groups were analysed with one-way ANOVA followed by Dunnett's post-hoc test. (*p<0.05, **p<0.01 vs. Control).

5.2.6. Effect of FGY-1153 on the interstitial fibrosis of heart and great vessels

The ANOVA analysis of interstitial fibrosis in SHR heart samples revealed no statistically significant difference between Control and Treatment groups (p=0.783). The collagen content however in WKY hearts was significantly lower (p=0.025) compared to the Control group (Mean area fractions ± SEM: WKY: 0.390±0.021; Control: 0.657±0.069; FGY120: 0.636±0.088; FGY400: 0.582±0.041; Fig. 11.). A statistically non-significant increase of vascular collagen could be observed in carotid arteries and aortas in Control group compared to WKY. No significant differences could be found between Control, FGY120 and FGY400 groups (Mean area fractions ± SEM: Aorta: WKY: 1.084±0.112 (p=0.536 vs. Control); Control: 1.378±0.414; FGY120: 1.239±0.526; FGY400: 1.458±0.324, (p=0.936); Carotid arteries: WKY: 4.860±0.532 (p=0.229 vs Control); Control: 5.994±0.660; FGY120: 5.745±1.465; FGY400: 5.158±1.097; (p=0.866), data not shown).

| A | B | C | D |
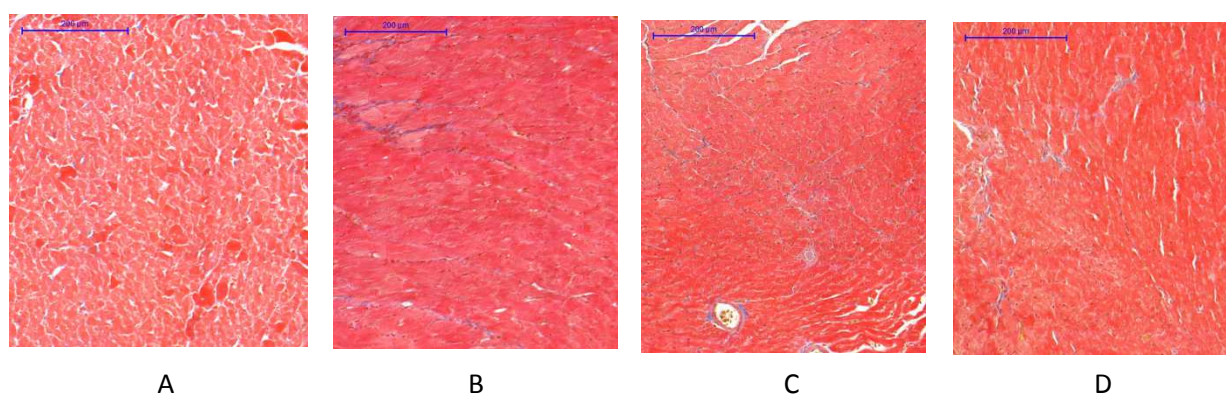
Fig. 11. Effect of FGY-1153 treatment on the interstitial cardiac fibrosis. Statistical analysis of Masson's trichrome stained sections revealed no significant difference between the Control (B), FGY120 (C) and FGY400 (D) groups. WKY group however showed significantly lower amount of collagen.

5.2.7. Effect of FGY-1153 on the intima-media thickness of great vessels

In comparison with the Control group (Fig. 12C), the intima-media thickness (IMT) of aorta was not altered significantly (p=0.718) neither in the FGY120 (Fig. 12C) nor in the FGY400 groups (Fig. 12D). IMT was however significantly smaller in WKY group (Fig. 12A) (p=0.0012 vs. Control).
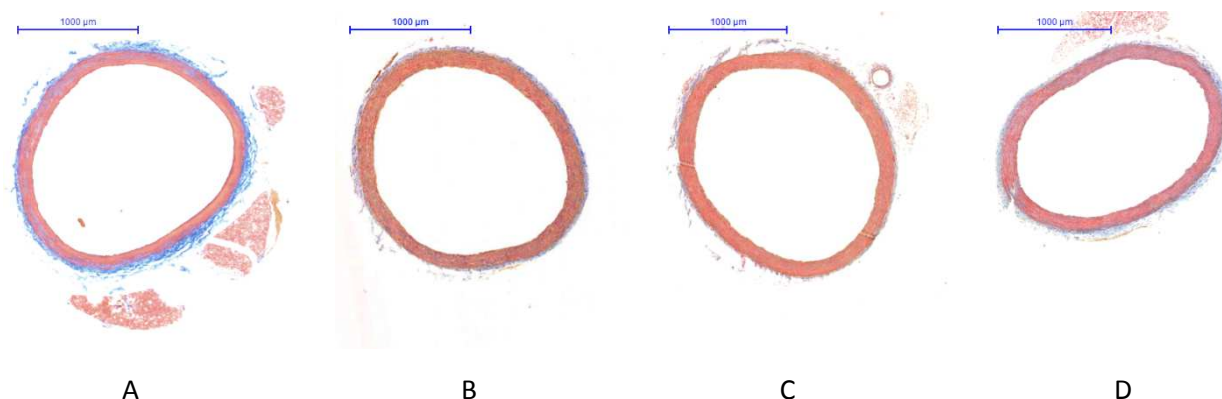
A B C D

Fig. 12. Masson's trichrome staining of aorta. IMT was the lowest in the WKY group (A). However in comparison with Control group (B), the IMT of aorta was not significantly altered in the FGY120 (C) and FGY400 groups (D).
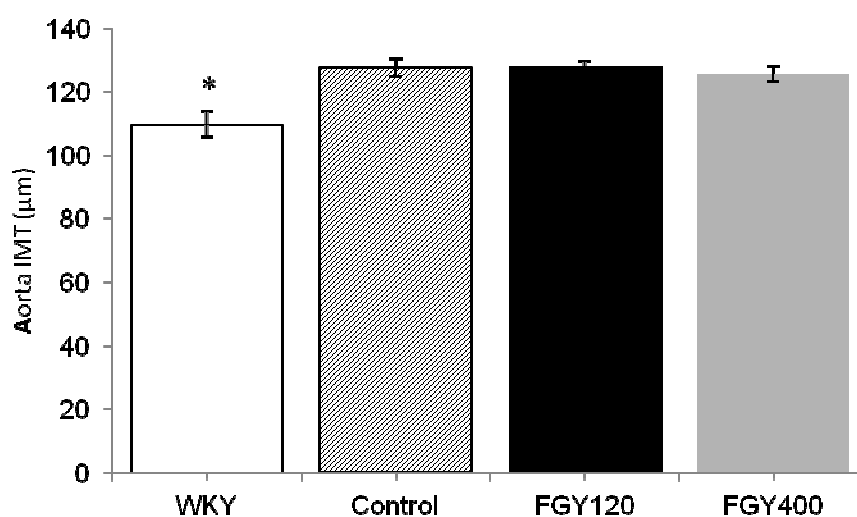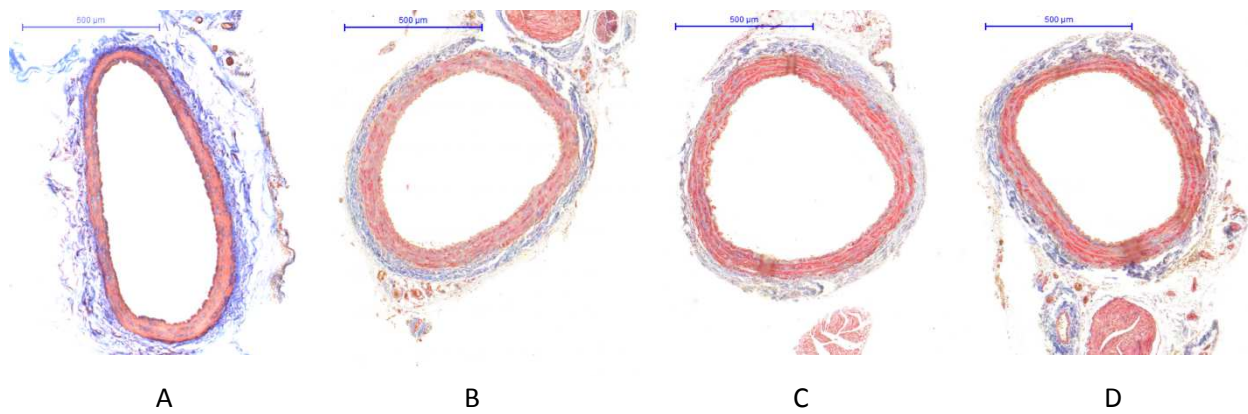

Fig. 13. Effect of FGY-1153 on the aortic intima-media thickness. (*p<0.05 vs. Control group).

In comparison with the Control group (Fig. 14), the intima-media thickness of carotid vessels was slightly decreased in both the FGY120 and FGY400 groups. However the alterations were not significant (p=0.149). The IMT of carotid arteries was the lowest in the WKY group (p=0.031 vs. Control).

Fig. 14. Masson's trichrome staining of carotid vessels. IMT was the lowest in the WKY group. In comparison with the Control group (B), the intima-media thickness of carotid vessels was slightly decreased in both the FGY120 (C) and FGY400 groups (D). The alterations were not significant.
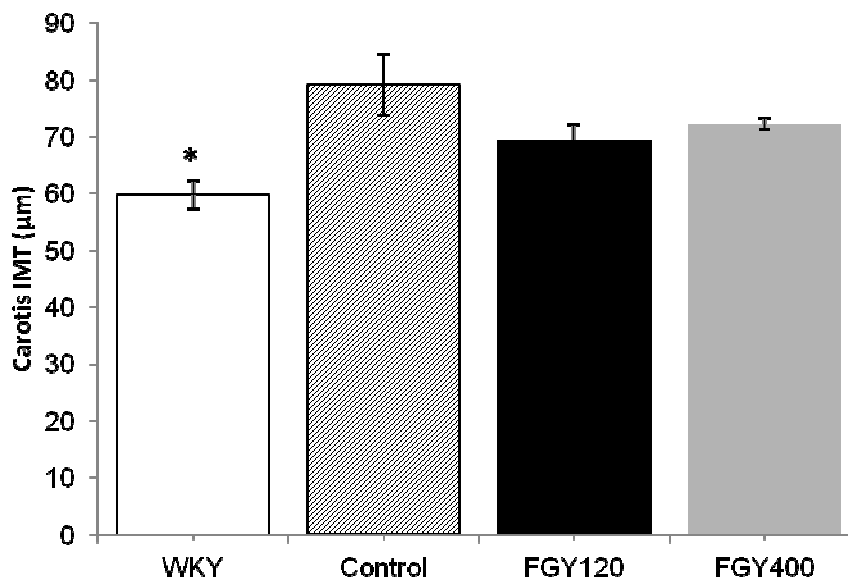
Fig. 15. Effect of FGY-1153 treatment on intima-media thickness of carotid vessels. ([*]p<0.05 vs. Control group).

5.2.8. Effect of FGY-1153 on the ultrastructural changes in myocardium and in great vessels

Electron microscopic studies of the myocardium

Transmission electron microscopic analysis of capillary endothelium in the myocardium (Fig.16.A-C,Fig.19.A-D) showed several cytoplasmic vesicles in all groups that can be the morphological sign of active vesicle transport from the extracellular matrix towards the capillary lumen.

In the cytoplasm glycogen (Fig.16. Fig.19. arrow heads) and lipid droplets (not shown) could be seen in all groups, however the amount of glycogen was slightly increased and the number of lipid droplets was slightly decreased in the FGY120 group compared to the Control and FGY400 (Fig.16.D-I) groups.

The morphology of Eberth' lines (not shown) and sarcomere units was normal in both the Control and the FGY-1153 treated groups (Fig.16.D-F).

The nuclei of cardiomyocytes in the Control rats display predominantly euchromatin with minor membrane-associated marginal heterochromatin (Fig.16.G). In contrast, in the other two groups cell nuclei were pale and displayed higher amount of membrane-associated marginal chromatin suggesting differences in the activity of synthesis (transcription) (Fig.16.H,I).

The mitochondria of SHR rats (Fig.16.D) differ from the normal mitochondria of healthy rats(Fig.19.D). In the Control group (Fig.16.J) extensive disruption of mitochondrial cristae and enlarged intracristal spaces could be observed. The mitochondrial population was characterized by morphological heterogeneity, their structure was polymorph, their shape was often elongated, and the mitochondrial matrix was very light.

The mitochondrial ultrastructure in the FGY120 group was similar to that of the healthy rats (Fig.16.K,Fig.19.D). The structure of the mitochondrial cristae was almost normal, dense matrix was seen and the mitochondria were less elongated. The ratio of mitochondria to myofibrils was higher, the elevated number of mitochondria was accompanied by increased amount of intracellular glycogen in comparison to the Control group. In Control group less and morphologically heterogenic mitochondrial population and less glycogen could be observed. Higher amount of mitochondria can produce more energy

for the contractile apparatus of the myocardium, thereby increasing the efficiency of energy utilization in the myocardium of the FGY120 rats.

In the samples of FGY400 group (Fig.16.L) the mitochondrial matrix was also dense, however more morphological abnormalities, e.g. disorganized mitochondrial cristae could be revealed in comparison to the FGY120 group.
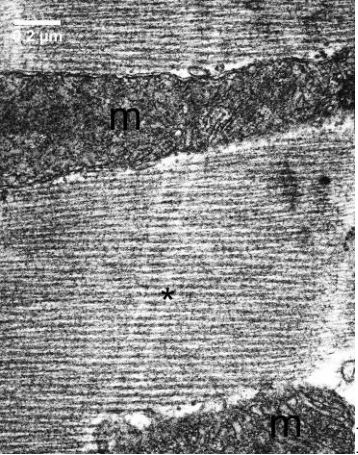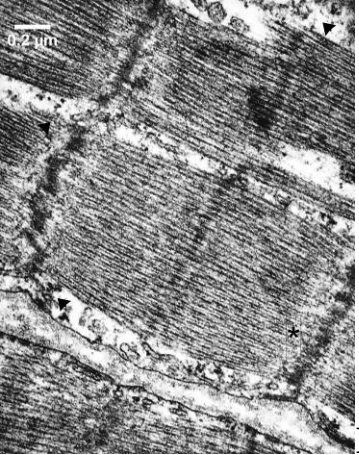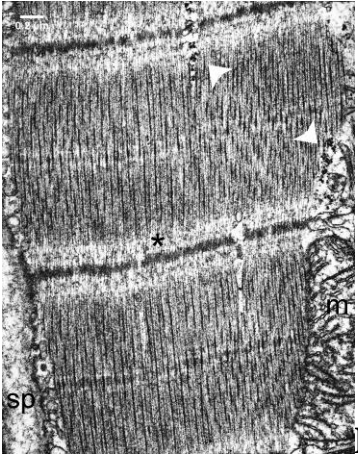
Control　　　　**FGY120**　　　　**FGY400**
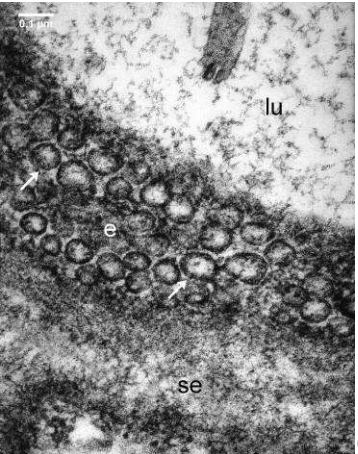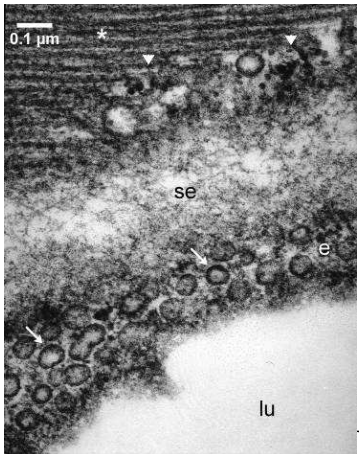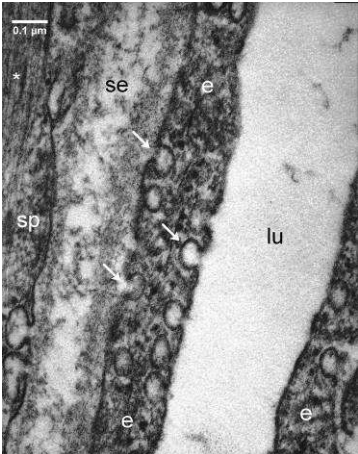
Control	FGY120	FGY400

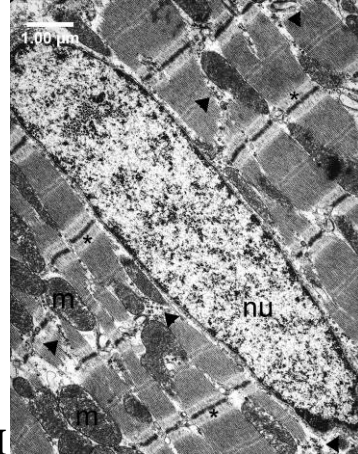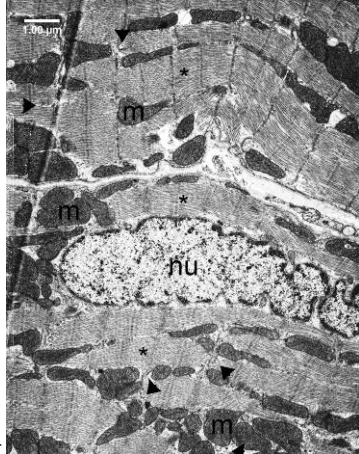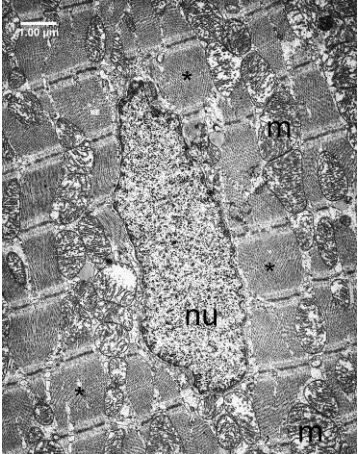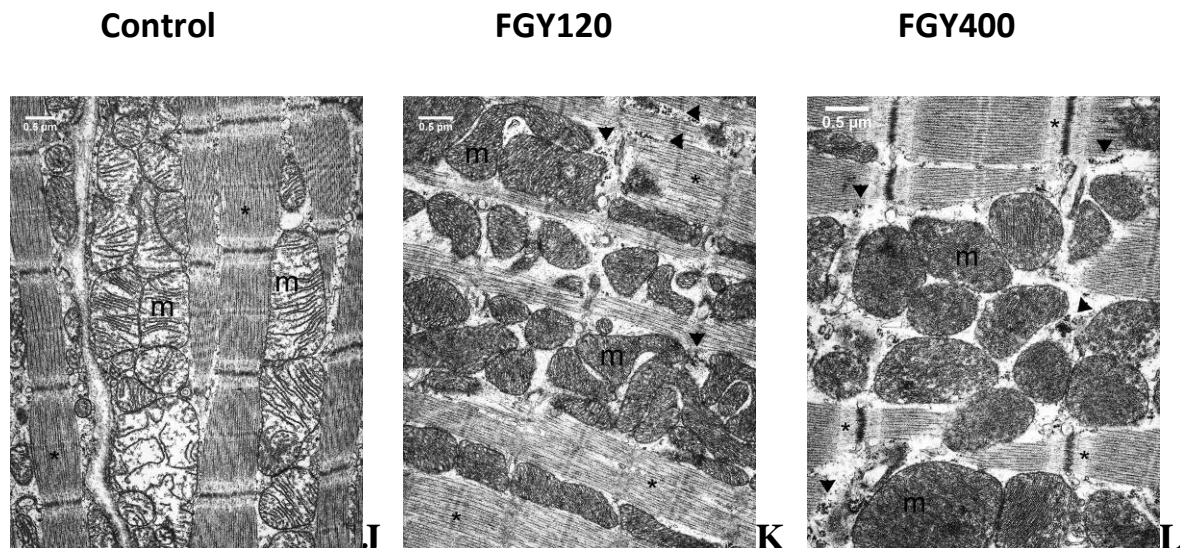**Fig. 16. Ultrastructural analysis of the cardiomyocytes in Control, FGY120 and FGY400 group.** Endothelium (e), Lumen of endothelium (lu), Subendothelium (se), Vesicles (arrows), Sarcoplasm (sp), Muscle fibers (*), Mitochondria (m), Nuclei (nu), Glycogen (arrow heads).

Electron microscopic studies of the walls of aortas and carotid arteries

The ultrastructure of the wall of normotensive aorta and carotid arteries is characterized by endothelial cells lying almost directly on the internal elastic lamina (Fig.20.,Fig.21.). The surface of the endothelial monolayer is smooth, the cells have very thin cytoplasm and an elongated nucleus which is oriented parallel to the internal elastic lamella. The subendothelial space is narrow, the internal elastic lamina is rarely interrupted. In the tunica intima the cellular elements (fibroblasts, smooth muscle cells) are arranged between the layers of internal elastic lamina(Fig.20.,Fig.21.).

In the aortic walls (Fig.17.) focal changes due to hypertension were observed in all hypertensive groups. There were no considerable ultrastructural differences between the groups.

In the carotid arteries (Fig.18.) the wall structure was pathologic similarly to the aortic walls.

The nuclei of smooth muscle cells in the intimal layer were lobular and sometimes highly active. The activated smooth muscle cells are involved in the synthesis of the components of fibers, which is confirmed by the presence of collagen and elastic fibers

around them (Fig. 17.-18.). Expanding smooth muscle cells sporadically broke through the internal elastic lamina (Fig.17. A,B,D,I; Fig.18. A,C,E,F), resulting in the appearance of collagen and cellular elements in the subendothelial space. Accumulation of connective tissue and cellular elements in the subendothelial space may have exerted tension to the endothelial monolayer, so the endothelial cells became distorted, their cytoplasm was lateralized and in some places became thinner. Presumably the endothelial permeability increased due to cell distortion, which contributed to subendothelial space expansion and further endothelial erosion.

Additional sign of tension-distorted endothelial cells is the altered orientation of their nuclei, which became rounded and protruded into the lumen, so the surface of the endothelial monolayer became rough (Fig.17. B,D,F,G; Fig.18. A,B,E).

Rearrangement of tunica media layers could be seen, as a consequence of hypertension-induced smooth muscle cell activation and collagen synthesis. In the walls of carotid arteries more intensive collagen synthesis was seen compared to aortic walls. We could not see any significant differences between the control group and the treated groups (FGY120 and FGY 400) (Fig.17.-18.).
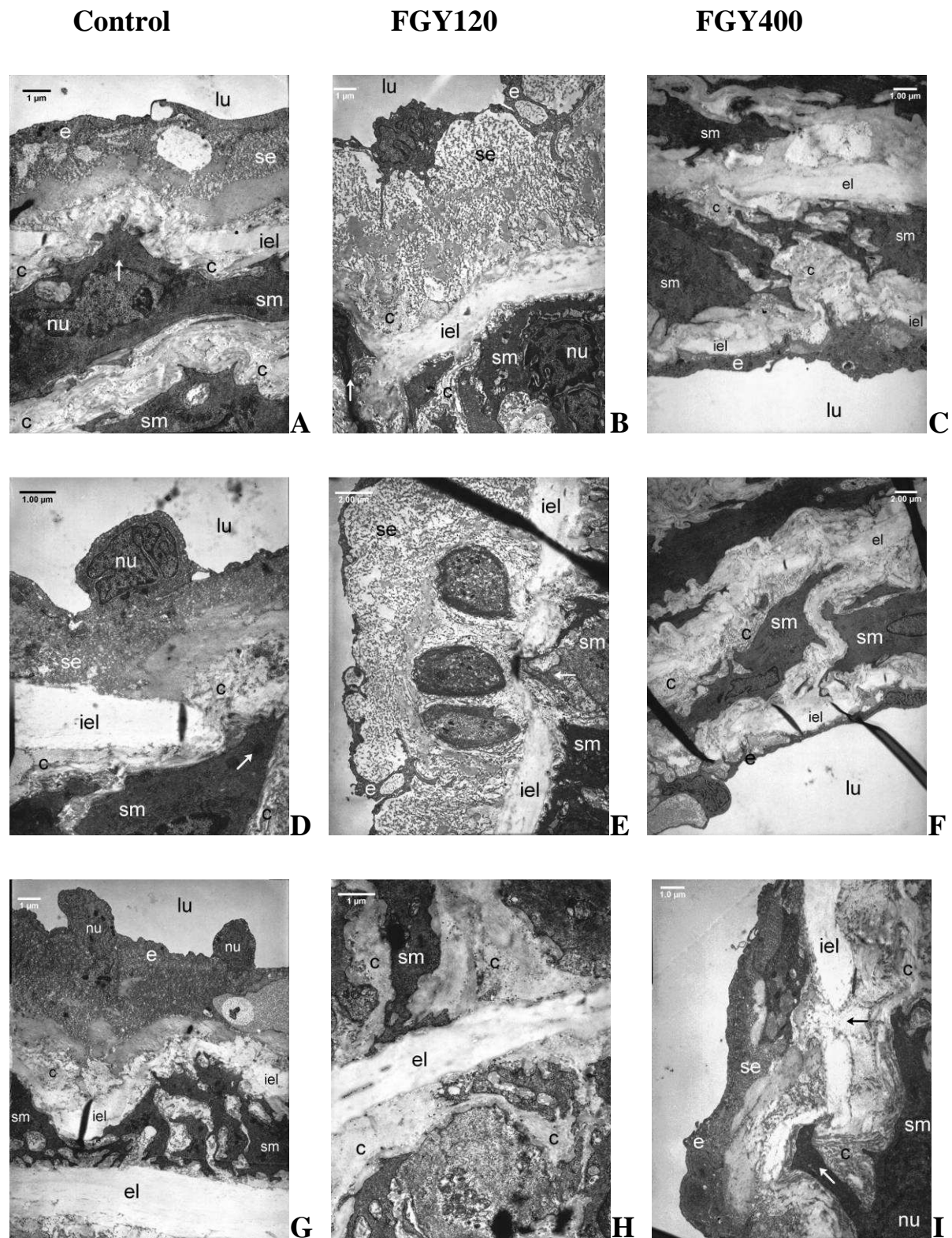
Control　　　**FGY120**　　　**FGY400**

Fig. 17. Ultrastructural analysis of the aortic wall of Control, FGY120 and FGY400 animals. Lumen (lu), Endothelium (e), Subendothelium (se), Internal elastic lamina (iel), Smooth muscle cells (sm), Collagen fibers (c), Interruption of internal elastic lamella by the smooth muscle cells (arrows).
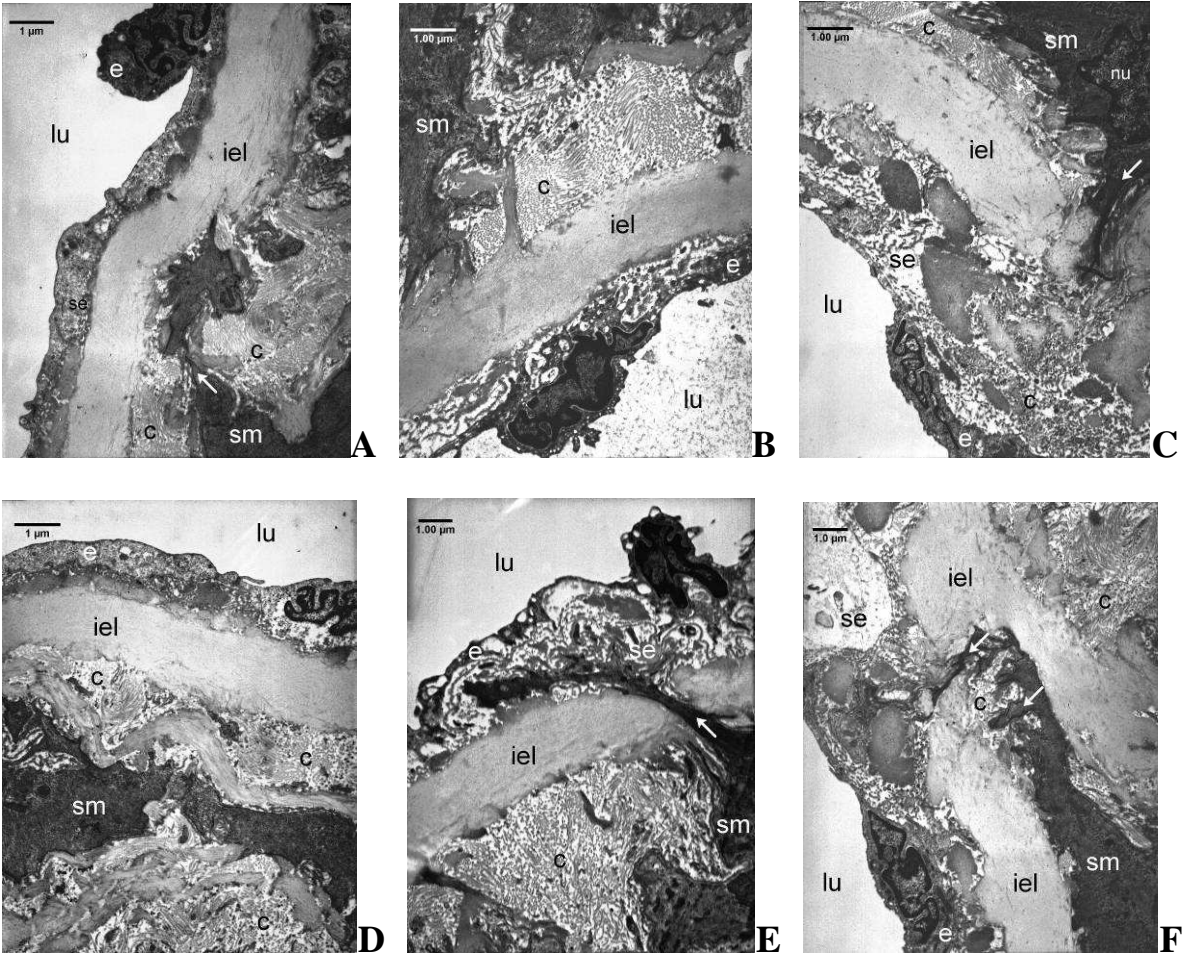
Control **FGY120** **FGY400**

Fig. 18. Ultrastructural analysis of the Control, FGY120 and FGY400 carotid walls. Lumen (lu), Endothelium (e), Subendothelium (se), Internal elastic lamina (iel), Smooth muscle cells (sm), Collagen fibers (c), Interruption of internal elastic lamella by the smooth muscle cells (arrows).
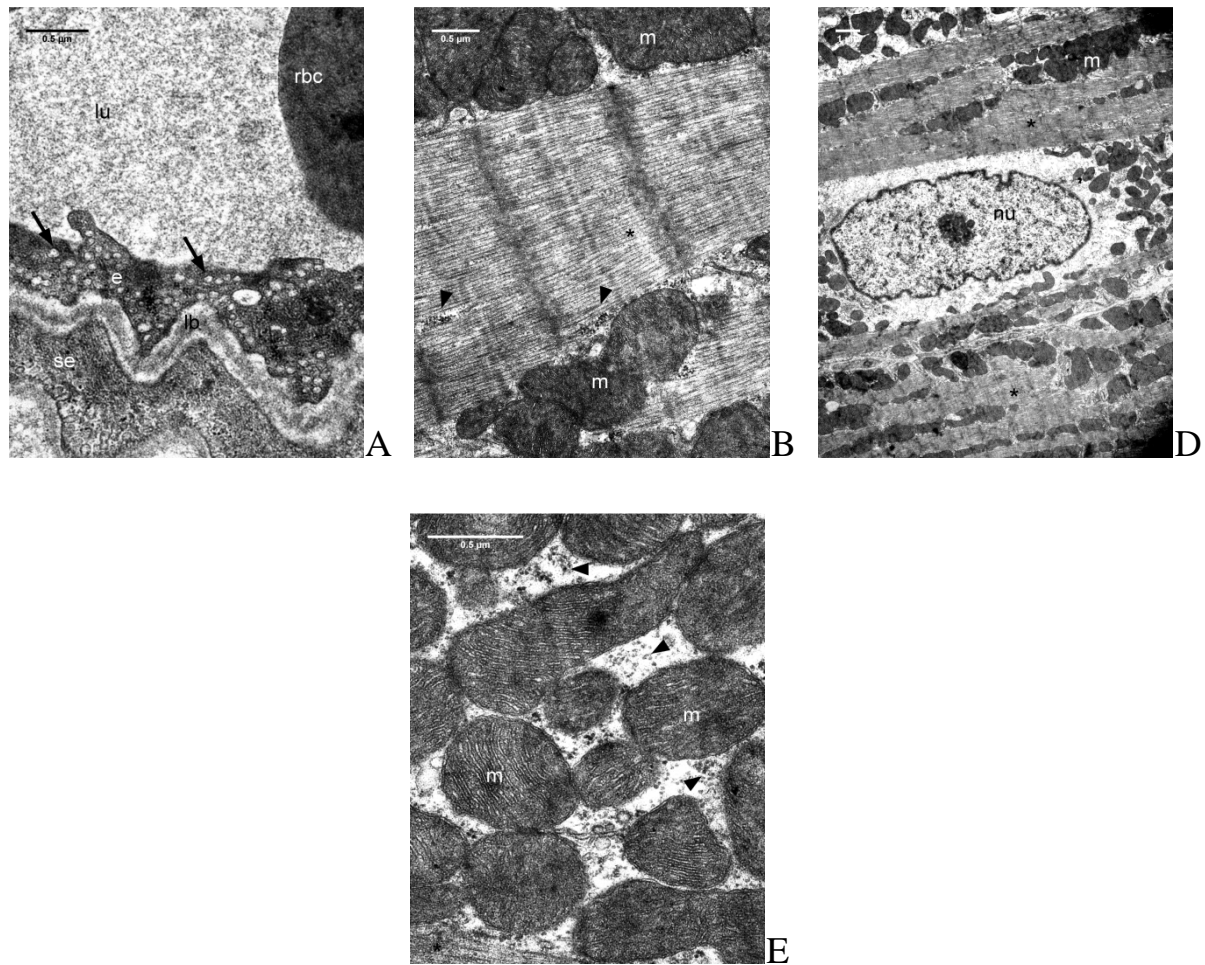
Fig. 19. Ultrastructural analysis of the cardiomyocytes in WKY group. Endothelium (e), Lumen of endothelium (lu), Subendothelium (se), Vesicles (arrows), Sarcoplasm (sp), Muscle fibers (*), Mitochondria (m), Nuclei (nu), Glycogen (arrow heads).
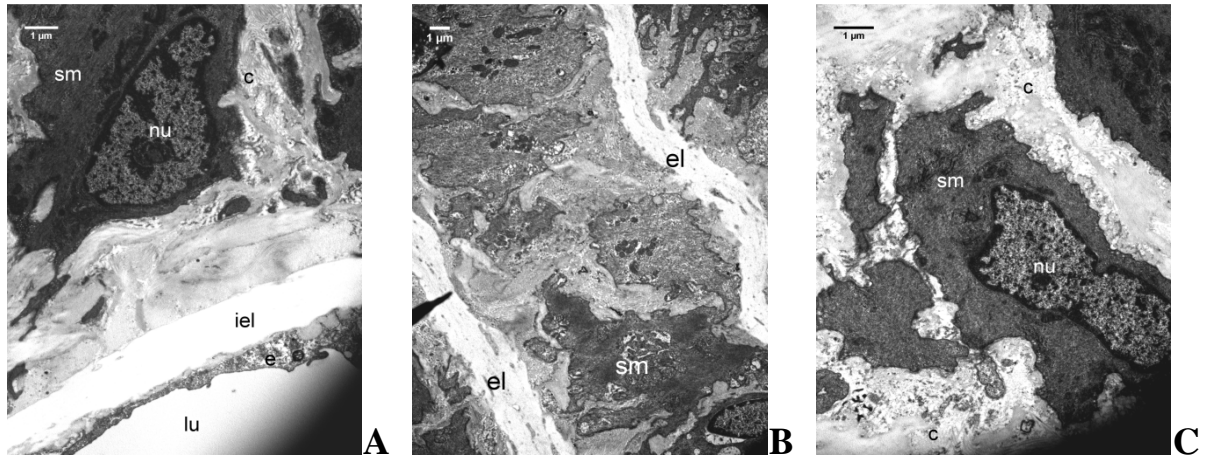
Fig. 20. Ultrastructural analysis of the aortic wall of WKY animals. Lumen (lu), Endothelium (e), Subendothelium (se), Internal elastic lamina (iel), Smooth muscle cells (sm), Collagen fibers (c), Interruption of internal elastic lamella by the smooth muscle cells (arrows).

Fig. 21. Ultrastructural analysis of the WKY carotid walls. Lumen (lu), Endothelium (e), Subendothelium (se), Internal elastic lamina (iel), Smooth muscle cells (sm), Collagen fibers (c), Interruption of internal elastic lamella by the smooth muscle cells (arrows).
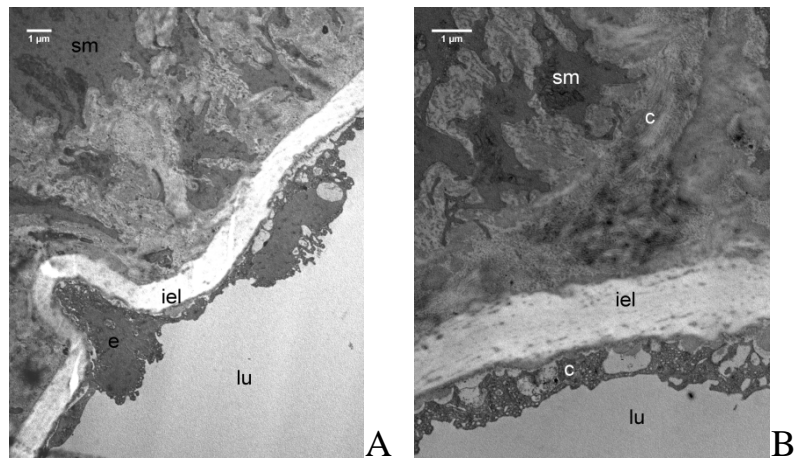
5.2.9. Effect of FGY-1153 on the TGFβ/SMAD2 signaling pathway in heart and great vessels

Western blot analysis of heart samples.

Fig. 22. The effect of FGY-1153 on the TGFβ/SMAD2 signaling pathway in heart samples. Western blot analysis showed that FGY-1153 treatment inhibited the cardiac expression of TGFβ and the phosphorylation of the SMAD2 protein in the FGY120 group, however the high dose treatment had no effect on the phosphorylation of SMAD2 in the FGY400 group. Actin is shown as loading control. Representative immunoblots from four experiments and densitometric evaluation are demonstrated. Data are presented as mean±S.E.M. Data were analysed with one-way ANOVA followed by Dunett's post-hoc test. *p<0.05, **p<0.01 vs. Control
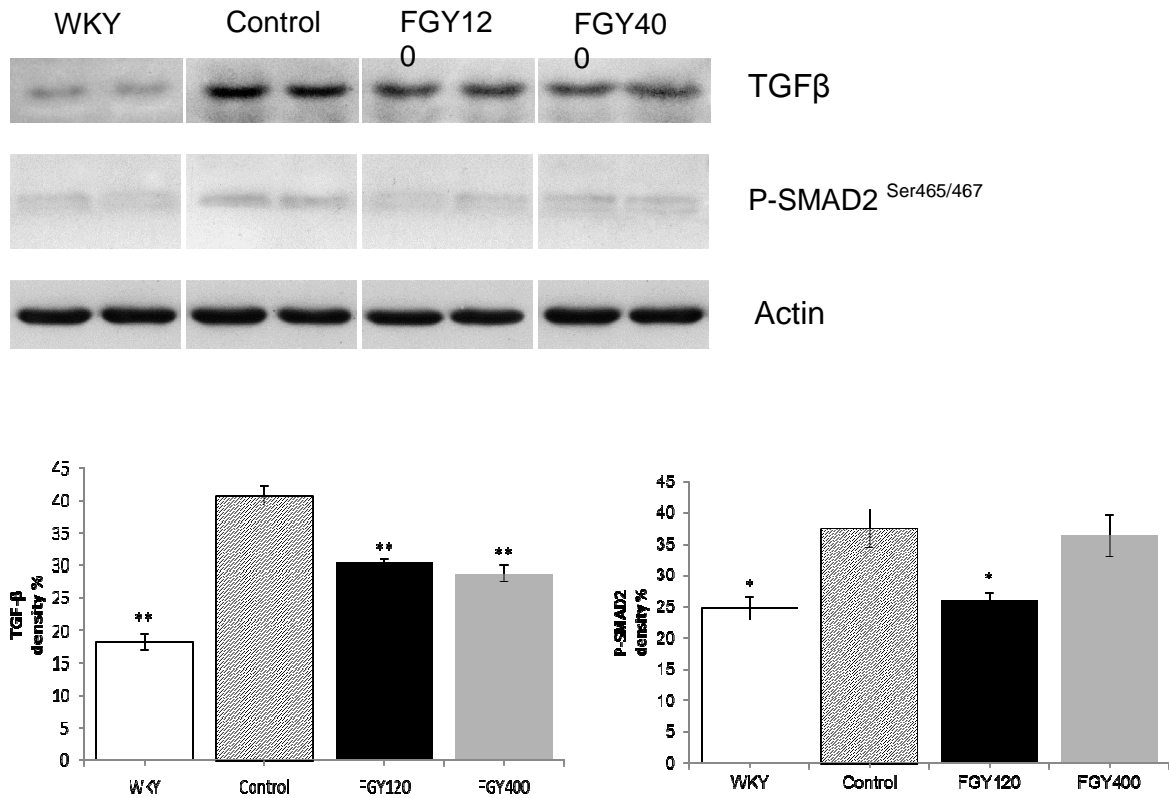
Western blot analysis of aorta samples.

Fig. 23. The effect of FGY-1153 on the TGFβ/SMAD2 signaling pathway in the aortic wall. Western blot analysis showed that low dose FGY-1153 treatment had no significant effect on the TGFβ expression, however the high dose treatment significantly inhibited the expression of TGFβ in the FGY400 group in comparison with both the Control and FGY120 group. The phosphorylation of the SMAD2 protein was significantly decreased in both the FGY120 and in FGY400 aortic samples. Actin is shown as loading control. Representative immunoblots from four experiments and densitometric evaluation are demonstrated. Data are presented as mean±S.E.M. Data were analysed with one-way ANOVA followed by Dunett's post-hoc test. *$p<0.05$, **$p<0.01$ vs. Control
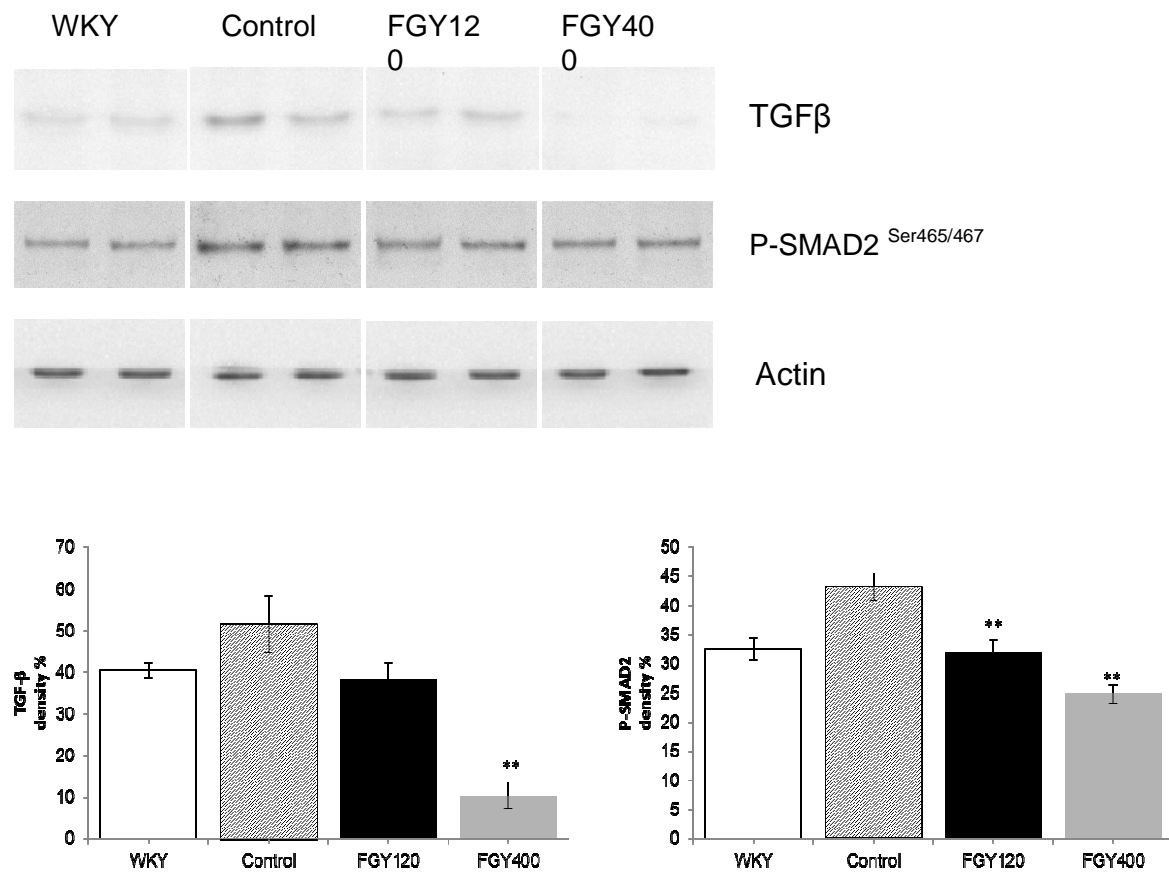
Western blot analysis of carotis samples.
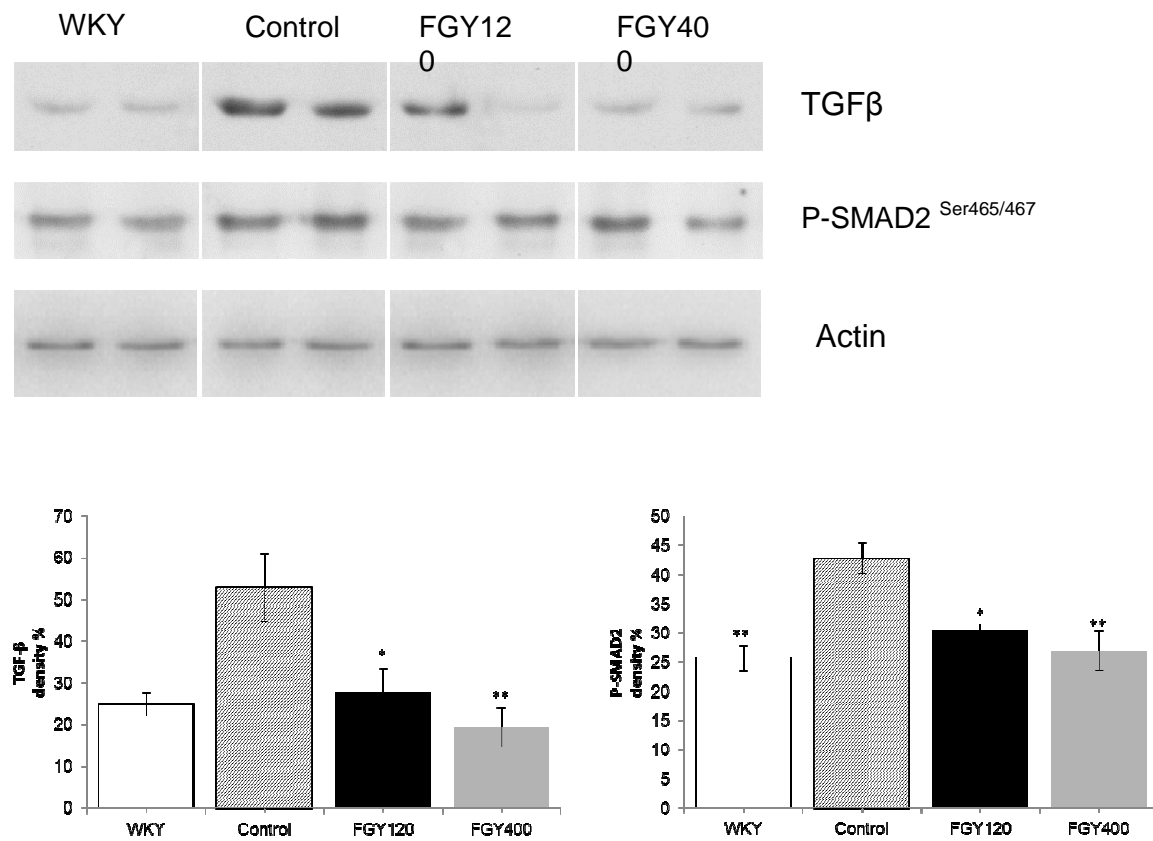
Fig. 24. The effect of FGY-1153 on the TGFβ/SMAD2 signaling pathway in the carotid arteries. Western blot analysis showed that both TGFβ expression and SMAD2 phosphorylation levels were significantly higher in Control group relative to WKY. Both high and low dose FGY-1153 treatment significantly inhibited the expression of TGFβ. The phosphorylation of the SMAD2 protein was significantly decreased in both the FGY120 and in FGY400 groups in carotid tissues. Actin is shown as loading control. Representative immunoblots from four experiments and densitometric evaluation are demonstrated. Data are presented as mean±S.E.M. Data were analysed by independent samples t-test between WKY and Control groups. Comparisons of Control and Treatment groups were made by one-way ANOVA followed by Dunnett's post-hoc test. $*p<0.05$, $**p<0.01$ vs. Control.

5.2.10. Effect of FGY-1153 on the phosphorylation of Akt/GSK-3β signaling cascade in heart and great vessels

Western blot analysis of heart samples
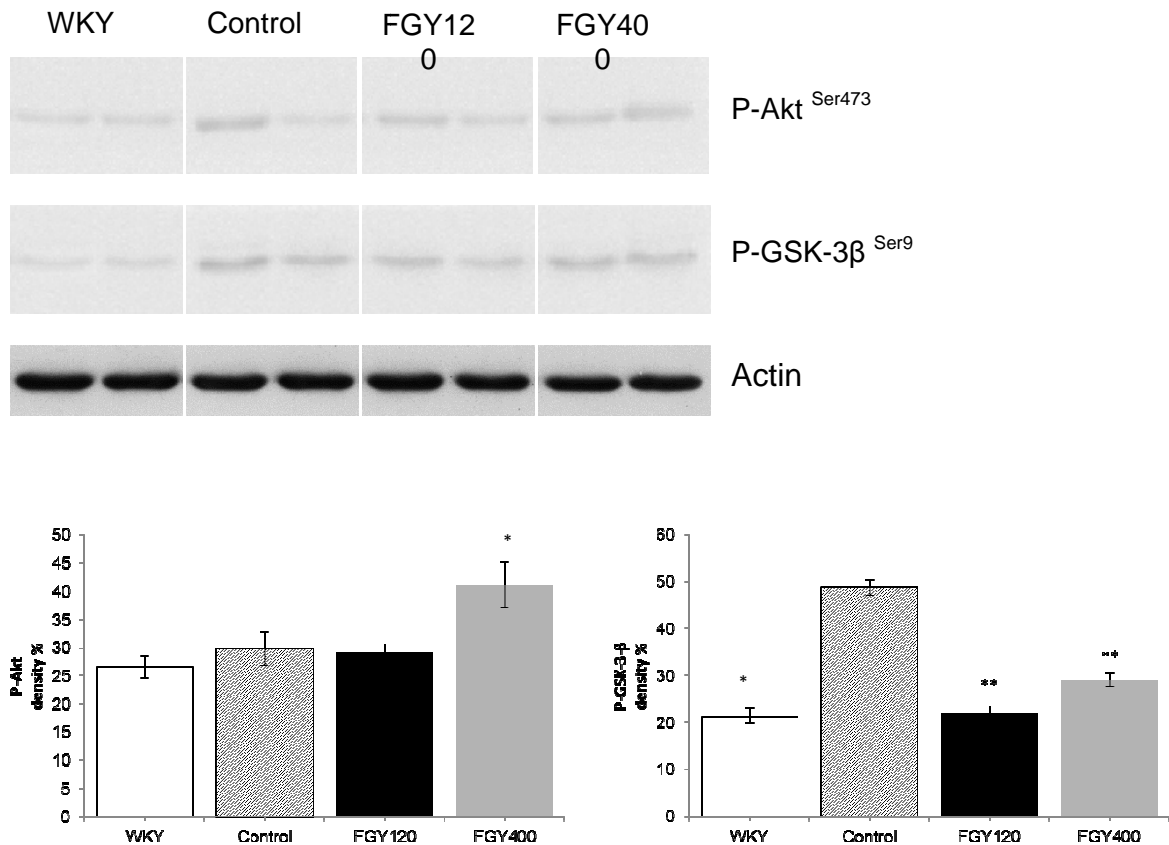
Fig. 25. The effect of FGY-1153 on the Akt/GSK-3β signaling cascade in heart samples. Western blot analysis showed GSK-3β phosphorylation to be significantly lower in WKY group relative to Control. High dose of FGY-1153 treatment significantly elevated phosphorylation of Akt protein, and both low dose and high dose treatment significantly attenuated the GSK-3β phosphorylation. Actin is shown as loading control. Representative immunoblots from four experiments and densitometric evaluation are demonstrated. Data are presented as mean±S.E.M. Data were analysed by independent samples t-test between WKY and Control groups. Comparisons of Control and Treatment groups were made by one-way ANOVA followed by Dunnett's post-hoc test. $*p<0.05$, $**p<0.01$ vs. Control.

Western blot analysis of aorta samples.
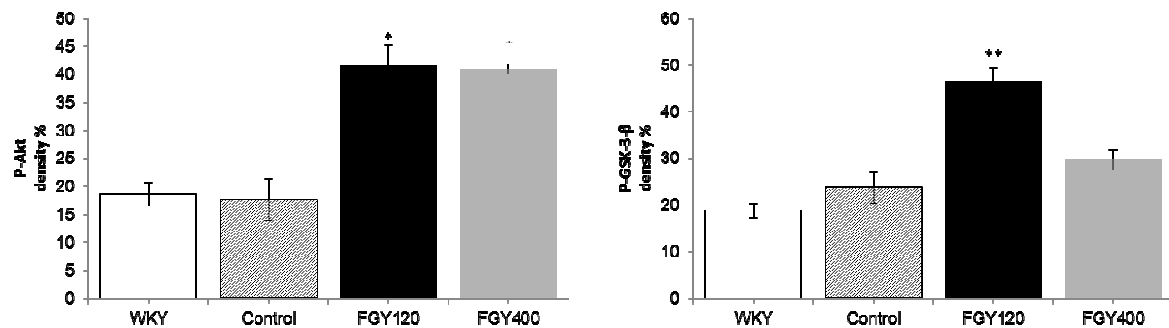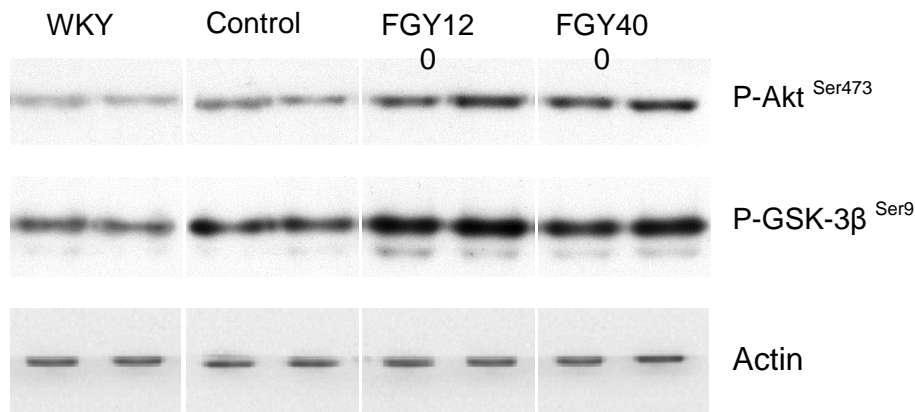
**Fig. 26. The effect of FGY-1153 on the Akt/GSK-3β signaling cascade in aortic wall.** Western blot analysis showed that FGY-1153 treatment significantly promoted the phosphorylation of Akt protein in the aortic tissues of both FGY120 and FGY400 groups, and the GSK-3β phosphorylation in the FGY120 group. However the high dose treatment had no effect on the GSK-3β phosphorylation in the FGY400 group. Actin is shown as loading control. Representative immunoblots from four experiments and densitometric evaluation are demonstrated. Data are presented as mean±S.E.M. Data were analysed by independent samples t-test between WKY and Control groups. Comparisons of Control and Treatment groups on GSK-3β data were made by one-way ANOVA followed by Dunnett's post-hoc test. On Akt data one-way ANOVA with Welch correction were conducted followed by Dunnett T3 post hoc test. *p<0.05, **p<0.01 vs. Control.

Western blot analysis of carotis samples.
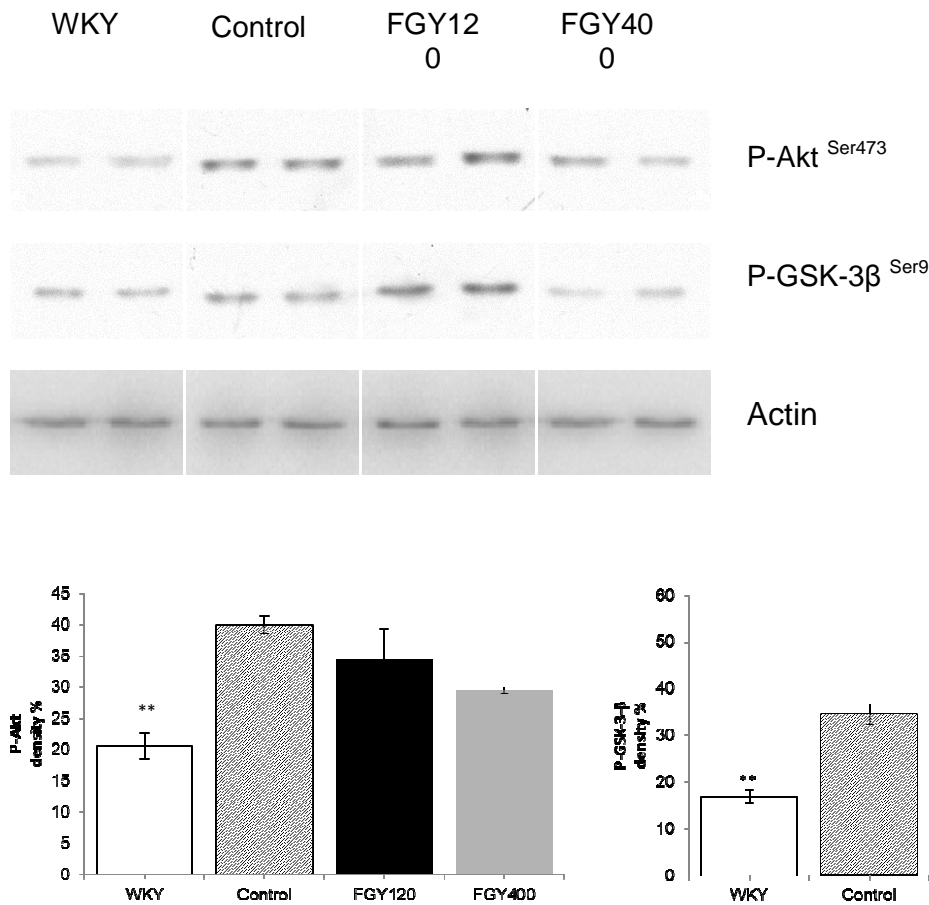
Fig. 27. The effect of FGY-1153 on the Akt/GK-3β signaling cascade in carotid vessels. Western blot analysis showed that phosphorylation level of both Akt and GSK-3β proteins were significantly higher in Control group relative to WKY. Low dose FGY-1153 treatment promoted while high dose treatment decreased the phosphorylation of GSK-3β protein, however it did not significantly influenced the Akt-1 phosphorylation in the carotid tissues of SHR rats. Actin is shown as loading control. Representative immunoblots from four experiments and densitometric evaluation are demonstrated. Data are presented as mean±S.E.M. Data were analysed by independent samples t-test between WKY and Control groups. Comparisons of Control and Treatment groups were made by one-way ANOVA followed by Dunnett's post-hoc test. *p<0.05, **p<0.01 vs. Control.

5.3. Discussion

The major finding of this study is that pharmacological inhibition of bradykinin B1 receptors did not cause significant elevation of blood pressure and did not cause worsening of hypertensive organ damages in a chronic hypertensive animal model. Moreover we have found that the administration of FGY-1153, an experimental bradykinin B1 receptor antagonist compound caused slight protective effect against the development of cardiac and vascular remodeling. We used the SHR which provides an animal model of high blood pressure that is similar to essential hypertension in humans (34).

Therefore we have examined the effect of FGY-1153, a bradykinin B1 receptor antagonist on the vascular and cardiac changes evoked by chronic hypertension. The FGY-1153 was administered orally in the food pellets at two concentrations (120 and 400 ppm).

FGY-1153 treatment did not have any effects on food consumption and on body weight. As a result of food consumption, the mean daily doses of FGY-1153 in the 120 ppm and 400 ppm groups were approximately 6 mg/kg and 20 mg/kg, respectively.

There was no significant difference between the blood pressures in the three groups, so FGY-1153 did not have antihypertensive effect. Despite the unchanged blood pressures, FGY-1153 had a mild but significant protective effect against the hypertension-induced left ventricular hypertrophy. The systolic left ventricular function - expressed as ejection fraction (EF) - decreased in the control group. In the FGY120 group however a significant improvement of EF could be seen, but in the high-dose group (FGY400) there was only an improving tendency in EF. The diastolic function (E/E' ratio), which is a more sensitive marker of heart function, improved similarly in both treatment groups.

In our SHR model, a slight vasoprotective effect of FGY-1153 treatment was also proved. Pharmacological inhibition of B1 receptors decreased the hypertension-induced vascular wall thickening in great vessels although these alterations were not significant (aorta and carotid artery), measured by a high-resolution ultrasound imaging system and by histological analysis.

The thickness of left ventricle and vascular walls are determined primarily by the amount of smooth muscle cells and by the amount of collagen content. The vascular collagen content was determined by transmission electron microscopy and by Masson's trichrome

staining. FGY-1153 treatment did not decrease significantly the extent of hypertension-induced myocardial and vascular fibrosis determined by the previously mentioned methods (64-66). Therefore the inhibition of cardiomyocyte and vascular smooth muscle cell hypertrophy was probably the main cause in the background of the decreased left ventricular and arterial wall thickness observed in FGY120 and FGY400 groups. The myocardial ultrastructure showed significant deterioration in untreated SHR animals (Control group). The mitochondrial structure was disorganized, the cristae were disrupted and the intracristal spaces were enlarged and the sizes of mitochondria were heterogenous. FGY-1153 treatment - predominantly the lower dose - decreased these unfavourable changes.

Hypertension-induced oxidative stress plays a central role in the pathogenesis of hypertensive organ damages (66-69). The consequences of the oxidative stress are vascular and cardiac remodeling, which is characterized by increased collagen accumulation and hypertrophy of smooth muscle cells.

In the mediation of vascular remodeling, the TGF-β/Smad pathway plays an important role (70). In the recent work we proved that FGY-1153 caused a significant inhibition in hypertension-induced activation of TGF and Smad-2 in both myocardium and vascular walls. Therefore in the background of the beneficial effects due to FGY-1153 treatment, the modulation of this pathway can be an important factor (32,71). Evaluating the most important cytoprotective mechanism - the Akt-1/GSK-3β pathway - we could not prove any unambiguous alterations.

6. CONCLUSIONS

In our study, we examined the effect of a PARP inhibitor (L-2286) in SHR at the stage of the development of LV hypertrophy. L-2286 exerted a beneficial effect on the progression of myocardial hypertrophy (thickness of PW and septum, RWT) and myocardial fibrosis. In the background of these changes, we did not observe any blood pressure lowering effect of PARP-inhibition. According to our results, PARP-inhibition can exert this antihypertrophic effect due to the activation of several prosurvival protein kinases (especially Akt-1/GSK-3β, FKHR, PKCε and Hsp90) and the inhibition of prohypertrophic (PKC- α/βII, - ζ/λ) protein kinases.

In conclusion, pharmacological inhibition of PARP-1 enzyme exerted significant protection against hypertensive cardiac remodeling in spite of the lack of having any antihypertensive effect. Therefore PARP can be a promising therapeutic target to prevent hypertensive cardiac complications even in those patients who do not reach the target blood pressure because of complaints or because of side effects caused by antihypertensive drug therapy. Our previous [36] and present results can introduce a new concept into the treatment of essential hypertension, namely to lower blood pressure to a more tolerable level and to prevent target organ damages by PARP-inhibition.

The long-term administration of the bradykinin B1 receptor antagonist compound FGY-1153 did not have any deleterious effects in SHR rats. Moreover we could observe some protective effect against the development of hypertensive cardiovascular remodeling despite that FGY-1153 did not have any antihypertensive effect. Inhibition of the TGF-β-Smad signaling may be the main underlying mechanism in the background of the cardiovascular protective effect.

7. ACKNOWLEDGEMENTS

8. REFERENCES

1. Hillege H.L., Girbes A.R., de Kam P.J., Boomsma F., de Zeeuw D., Charlesworth A., et al., Renal function, neurohormonal activation, and survival in patientswith chronic heart failure, Circulation 102 (2000) 203–210.
2. Deedwania P.C., Blood pressure control in diabetes mellitus: is lower always better, and how low should it go? Circulation 123 (2011) 2776–2778.
3. Qiu C., Winblad B., Fratiglioni L., The age-dependent relation of blood pressure to cognitive function and dementia, Lancet Neurol. 4 (2005) 487–499.
4. Birns J., Markus H., Kalra L., Blood pressure reduction for vascular risk: is there a price to be paid? Stroke 36 (2005) 1308–1313.
5. Dikalov S., Cross talk between mitochondria and NADPH oxidases, Free Radic. Biol. Med. 51 (2011) 1289–1301.
6. van Eickels M, Schreckenberg R, Doevendans PA, Meyer R, Grohé C, Schlüter KD. The influence of oestrogen-deficiency and ACE inhibition on the progression of myocardial hypertrophy in spontaneously hypertensive rats. Eur J Heart Fail (2005) 7:1079-1084.
7. Smith PG, Poston CW, Mills E. Ontogeny of neural and non-neural contributions to arterial blood pressure in spontaneously hypertensive rats. Hypertension (1984) 6: 54 60.
8. Bing OHL, Conrad CH, Boluyt MO, Robinson KG, Brooks WW. Studies of prevention, treatment and mechanisms of heart failure in the aging spontaneously hypertensive rat. Heart Fail Rev (2002) 7:71-88.
9. Boluyt MO, Bing OHL. Matrix gene expression and decompensated heart failure: The aged SHR model. Cardiovasc Res (2000) 46:239-249. Review.
10. Drummond G.R., Selemidis S., Griendling K.K., Sobey C.G., Combating oxidative stress in vascular disease: NADPH oxidases as therapeutic targets, Nat. Rev. Drug Discov. 10 (2011) 453–471.
11. Birns J., Markus H., Kalra L., Blood pressure reduction for vascular risk: is there a price to be paid? Stroke 36 (2005) 1308–1313.
12. Bogoyevitch MA. Signalling via stress-activated mitogen-activated protein kinases in the cardiovascular system. Cardiovasc Res (2000)45:826-842.
13. Koide Y, Tamura K, Suzuki A, Kitamura K, Yokoyama K, Hashimoto T, hirawa N, Kihara M, Ohno S, Umemura S. Differential induction of protein kinase C isoforms at the cardiac hypertrophy stage and congestive heart failure stage in Dahl Salt-Sensitive rats. Hypertens Res (2003) 26:421-426.
14. Luedde M, Katus HA, Frey N. Novel molecular tergets in the treatment of cardiac hypertrophy. Recent Patents on Cardiovasc Drug Discov (2006) 1:1-20.
15. Tapodi A, Debreceni B, Hanto K, Bognar Z, Wittmann I, Gallyas F Jr, Varbiro G, Sumegi B. Pivotal role of Akt activation in mitochondrial protection and cell survival by poly(ADP-ribose)polymerase-1 inhibition in oxidative stress. J Biol Chem (2005)280:35757-35775.
16. Kovacs K, Toth A, Deres P, Kalai T, Hideg K, Gallyas F Jr, Sumegi B. Critical role of PI3-kinase/Akt activation in the PARP inhibitor induced heart function recovery during ischemia-reperfusion. Biochem Pharmacol (2006)71:441-452.
17. Escobales N., Crespo M.J. Oxidative-nitrosative stress in hypertension Curr. Vasc. Pharmacol., 3 (2005) 231–246

18. Xie J.J., Yu X., Liao Y.H., Chen J., Yao R. *et al.* Poly (ADP-Ribose) polymerase inhibition attenuates atherosclerotic plaque development in ApoE-/- mice with hyperhomocysteinemia J. Atheroscler. Thromb., 16 (2009) 641–653

19. Csiszar A., Pacher P., Kaley G., Ungvari Z. Role of oxidative and nitrosative stress, longevity genes and poly(ADP-ribose) polymerase in cardiovascular dysfunction associated with aging Curr. Vasc. Pharmacol., 3 (2005) 285–291

20. Briones A.M., Touyz R.M. Oxidative stress and hypertension: current concepts Curr. Hypertens. Rep., 12 (2010) 135–142

21. Wincewicz A., Sulkowska M., Rutkowski R., Sulkowski S., Musiatowicz B. *et al.* STAT1 and STAT3 as intracellular regulators of vascular remodeling Eur. J. Intern. Med., 18 (2007) 267–271

22. Castier Y., Ramkhelawon B., Riou S., Tedgui A., Lehoux S. Role of NF-kappaB in flow-induced vascular remodeling Antioxid. Redox Signal., 11 (2009) 1641–1649

23. Washida K., Ihara M., Nishio K., Fujita Y., Maki T. *et al.* Nonhypotensive dose of telmisartan attenuates cognitive impairment partially due to peroxisome proliferator-activated receptor-gamma activation in mice with chronic cerebral hypoperfusion Stroke, 41 (2010) 1798–1806

24. Euler-Taimor G, Heger J. The complex pattern of SMAD signaling in the cardiovascular system. Cardiovasc Res (2006) 69:15–25.

25. Khan R, Sheppard R. Fibrosis in heart disease: understanding the role of transforming growth factor-beta in cardiomyopathy, valvular disease and arrhythmia. Immunology (2006)118:10–4.

26. Leask A, Abraham DJ. TGF-β signaling and the fibrotic response. FASEB J (2004) 18:816–7.

27. Verrecchia F, Mauviel A. Transforming growth factor-beta signaling through the Smad pathway: role in extracellular matrix gene expression and regulation. J Invest Dermatol (2002)118:211–5.

28. Ikedo H, Tamaki K, Ueda S, Kato S, Fujii M, Ten Dijke P, et al. Smad protein and TGF-β signaling in vascular smooth muscle cells. Int J MolMed (2003)11:645–50.

29. Szabó Cs, Pacher P, Zsengellér Zs, Vaslin A, Komjáti K, Benkö R, et al. Angiotensi II-mediated endothelial dysfunction: role of poly(ADP-ribose) polymerase activation. Mol Med (2004) 10:28-35.

30. Pacher P, Mabley JG, Soriano FG, Liaudet L, Szabó C. Activation of poly(ADP-ribose) polymerase contributes to the endothelial dysfunction associated with hypertension and aging. Int J Mol Med (2002) 9:659-664.

31. Palfi A, Toth A, Hanto K, Deres P, Szabados E, Szereday Z, et al. PARP inhibition prevents postinfarction myocardial remodeling and heart failure via the protein kinase C/glycogen synthase kinase-3β pathway. J Mol Cell Cardiol (2006) 41:149-159.

32. Bartha E, Solti I, Kereskai L, Lantos J, Plozer E, Magyar K, et al. PARP inhibition delays transition of hypertensive cardiopathy to heart failure in spontaneously hypertensive rats. Cardiovasc Res (2009) 83:501-510.

33. Racz B, Hanto K, Tapodi A, Solti I, Kalman N, Jakus P, et al. Regulation of MKP-1 expression and MAPK activation by PARP-1 in oxidative stress: a new mechanism for the cytoplasmic effect of PARP-1 activation. Free Radic Biol Med (2010) 49:1978-1988.

34. Ito N, Ohishi M, Yamamoto K, Tatara Y, Shiota A, Hayashi N, et al. Renin-Angiotensin inhibition reverses advanced cardiac remodeling in aging spontaneously hypertensive rats. Am J Hypertens (2007)20:792-799.

35. Kokubo M, Uemura A, Matsubara T, Murohara T. Noninvasive evaluation of the time course of change in cardiac function in spontaneously hypertensive rats by echocardiography. Hypertens Res (2005) 28:601-609.

36. Meurrens K, Ruf S, Ross G, Schleef R, van Holt K, Schlüter KD. Smoking accelerates the progression of hypertension-induced myocardial hypertrophy to heart failure in spontaneously hypertensive rats. Cardiovasc Res (2007)76:311-322.

37. Deedwania PC. Blood pressure control in diabetes mellitus: is lower always better, and how low should it go? Circulation. (2011) 123(24): 2776-8.

38. Pavlicević I, Kuzmanić M, Rumboldt M, Rumboldt Z. Interaction between antihypertensives and NSAIDs in primary care: a controlled trial. Can J Clin Pharmacol. 15; (2008) 372-82.

39. Tschöpe C, Heringer-Walther S, Walther T. Regulation of the kinin receptors after induction of myocardial infarction: a mini-review. Braz J Med Biol Res. 33 (2000) 701–8:

40. Leeb-Lundberg LM, Marceau F, Muller-Esterl W, Pettibone DJ, Zuraw BL. International union of pharmacology. XLV. Classification of the kinin receptor family: from molecular mechanisms to pathophysiological consequences. Pharmacol Rev. 57(2005) 27–77

41. Golias Ch, Charalabopoulos A, Stagikas D, Charalabopoulos K, Batistatou A. The kinin system–bradykinin: biological effects and clinical implications. Multiple role of the kinin system–bradykinin. Hippokratia. (2007) 11; 124–8.

42. Pfeffer J M, Pfeffer M A, Mirsky I, and Braunwald E Regression of left ventricular hypertrophy and prevention of left ventricular dysfunction by captopril in the spontaneously hypertensive rat. Proc Natl Acad Sci U S A. (1982) 79(10):3310-4.

43. Lip GY, Felmeden DC, Li-Saw-Hee FL, Beevers DG. Hypertensive heart disease. A complex syndrome or a hypertensive 'cardiomyopathy'? Eur Heart J (2000) 21:1653-1665.

44. Pacher P, Szabo C. Role of the peroxynitrite-poly(ADP-ribose) polymerase pathway in human disease. Am J Pathol (2008) 173:2-13.

45. McCrossan ZA, Billeter R, White E. Transmural changes in size, contractile and electrical properties of SHR left ventricular myocytes during compensated hypertrophy. Cardiovasc Res (2004) 63:283-292.

46. Pálfi A, Tóth A, Kulcsár G, Hantó K, Deres P, Bartha E, et al. The role of Akt and MAP kinase systems in the protective effect of PARP inhibition in Langendorff perfused and in isoproterenol-damaged rat hearts. J Pharmacol Exp Ther (2005) 315:273-282.

47. Taniike M, Yamaguchi O, Tsujimoto I, Hikoso S, Takeda T, Nakai A, et al. Apoptosis signal-regulating kinase 1/p38 signaling pathway negatively regulates physiological hypertrophy. Circulation (2008) 117:545-552.

48. Li HH, Willis MS, Lockyer P, Miller N, MCDonough H, Glass DJ, Patterson C. Atrogin-1 inhibits Akt-dependent cardiac hypertrophy in mice via ubiquitin-dependent coactivation of Forkhead proteins. J Clin Invest (2007) 117:3211-3223.

49. Ni YG, Berenji K, Wang N, Oh M, Sachan N, Dey A, et al. Foxo transcription factors blunt cardiac hypertrophy by inhibiting calcineurin signaling. Circulation (2006) 114:1159-1168

50. Sőti Cs, Nagy E, Giricz Z, Vígh L, Csermely P, Ferdinandy P. Heat shock proteins as emerging therapeutic targets. Br J Pharmacol (2005)146:769-780.

51. Jiang B, Xiao W, Shi Y, Liu M, Xiao X. Heat shock pretreatment inhibited the release of Smac/DIABLO from mitochondria and apoptosis induced by hydrogen peroxide in cardiomyocytes and C_2C_{12} myogenic cells. Cell Stress Chaperons (2005) 10:252-262.

52. Shinohara T, Takahashi N, Kohno H, Yamanaka K, Ooie T, Wakisaka O, et al. Mitochondria are targets for geranylgeranylacetone-induced cardioprotection against ischemia-reperfusion in rat heart. Am J Physiol Heart Circ Physiol (2007) 293:H1892-H1899.

53. Pacher P, Szabó C. Role of poly(ADP-ribose) polymerase 1 (PARP-1) in cardiovascular diseases: The therapeutic potential of PARP inhibitors. Cardiovasc Drug Rev (2007) 25:235-260.

54. Wang Y. Mitogen-Activated Protein Kinases in heart development and diseases. Circulation (2007) 116:1413-1423.Review

55. Kacimi R, Gerdes AM. Alterations in G protein and MAP Kinase signaling pathways during cardiac remodeling in hypertension and heart failure. Hypertension (2003) 41:968-977.

56. Liang Q, Molkentin JD. Redefining the roles of p38 and JNK signaling in cardiac hypertrophy: dichotomy between cultured myocytes and animal models. J Mol Cell Cardiol (2003) 35:1385-1394. Review

57. Dorn II GW, Force T. Protein kinase cascades in the regulation of cardiac hypertrophy. J Clin Invest (2005) 115:527-537. Review

58. Carlota García-Hoz, Guzmán Sánchez-Fernández, Ramón García-Escudero, María Fernández-Velasco, Julia Palacios-García, Marisol Ruiz-Meana, et al. Protein Kinase C (PKC)ζ-mediated $G\alpha_q$ Stimulation of ERK5 Protein Pathway in Cardiomyocytes and Cardiac Fibroblasts JBiolChem. (2012) 287:7792–7802.

59. Braz JC, Bueno OF, De Windt LJ, Molkentin JD. PKC alpha regulates the hypertrophic growth of cardiomyocytes through extracellular signal-regulated kinase1/2 (ERK1/2) J. Cell Biol. (2002) 156:905–919.

60. Takeishi Y, Chu G, Kirkpatrick D M, Li Z, Wakasaki H, Kranias E G, King G L, and Walsh R A In vivo phosphorylation of cardiac troponin I by protein kinase Cbeta2 decreases cardiomyocyte calcium responsiveness and contractility in transgenic mouse hearts. J Clin Invest. (1998) 102: 72–78.

61. Inagaki K, Iwanaga Y, Sarai N, Onozawa Y, Takenaka H, Mochly-Rosen D, Kihara Y. Tissue angiotensin II during progression or ventricular hypertrophy to heart failure in hypertensive rats; differential effects on PKC epsilon and PKC beta. J Mol Cell Cardiol. (2002) 34:1377-1385.

62. Dorn II GW, Souroujon MC, Liron T, Chen CH, Gray MO, Zohu HZ, et al. Sustained in vivo cardiac protection by a rationally designed peptide that causes epsilon protein kinase C translocation. Proc Natl Acad Sci USA (1999) 96: 12798–12803,.

63. Steinberg R, Harari OA, Lidington EA, Boyle JJ, Nohadani M, Samarel AM, et al. A protein kinase Cepsilon-anti-apoptotic kinase signalling complex protects human vascular endothelial cells against apoptosis through induction of Bcl-2. J Biol Chem (2007) 282:32288-32297.

64. Limas C, Westrum B, Limas CJ. The evolution of vascular changes in the spontaneously hypertensive rat. Am J Pathol. 1980 February; 98(2): 357–384.

65. Sandow SL, Gzik DJ, Lee RM. Arterial internal elastic lamina holes: relationship to function? J Anat. (2009) 214: 258-66 .

66. Okruhlicová L, Dlugosová K, Mitasíková M, Bernátová I. Ultrastructural characteristics of aortic endothelial cells in borderline hypertensive rats exposed to chronic social stress. Physiol Res. 57 (2008) Suppl 2: S31-7.

67. Cal LA, Maso LD, Caielli P, Pagnin E, Fusaro M, Davis PA, Pessina AC. Effect of olmesartan on oxidative stress in hypertensive patients: mechanistic support to clinical trials derived evidence. Blood Press. 20 (2011) 376-82

68. Puddu P, Puddu GM, Cravero E, Rosati M, Muscari A. The molecular sources of reactive oxygen species in hypertension. Blood Press (2008) 17:70–77.
69. Koichi Tanaka, Masaaki Honda, Toshikazu Takabatake. Redox Regulation of MAPK Pathways and Cardiac Hypertrophy in Adult Rat Cardiac Myocyte. JACC. 37 (2001) 676-685.
70. Ruiz-Ortega M, Rodríguez-Vita J, Sanchez-Lopez E, Carvajal G, Egido J. TGF-β signaling in vascular fibrosis. Cardiovasc Res 74 (2007) 196-206.
71. Perrotta I, Brunelli E, Sciangula A, Conforti F, Perrotta E, Tripepi S, Donato G, Cassese M. iNOS induction and PARP-1 activation in human atherosclerotic lesions: an immunohistochemical and ultrastructural approach. Cardiovasc Pathol. (2011) 20(4):195-203.

9. PUBLICATIONS OF THE AUTHOR

MOLNÁR L, KISZLER G, POLLÁK E, <u>DERES L;</u> Distribution pattern of γ-amino butyric acid immunoreactive neural structures in the central and peripheral nervous system of the tubificid worm, Limnodrilus hoffmeisteri. *Hydrobiologia* 564**:**(1) *pp. 33-43.* (2006) IF: 1.985

MAGYAR K, <u>DERES L,</u> EROS K, BRUSZT K, SERESS L, HAMAR J, HIDEG K, BALOGH A, GALLYAS F JR, SUMEGI B, TOTH K, HALMOSI R; A quinazoline-derivative compound with PARP inhibitory effect suppresses hypertension-induced vascular alterations in spontaneously hypertensive rats. *Biochim Biophys Acta.* 19;1842(7):935-944. [Epub ahead of print] (2014) IF: 4.91

<u>DERES L</u>, BARTHA E, PALFI A, EROS K, RIBA A, LANTOS J, KALAI T, HIDEG K, SUMEGI B, GALLYAS F, TOTH K, HALMOSI R; PARP-inhibitor treatment prevents hypertension induced cardiac remodeling by favorable modulation of heat shock proteins, Akt-1/GSK-3β and several PKC isoforms. *PLoS One*; 9(7): e102148. doi:10.1371/journal.pone.0102148 (2014) IF: 3.73

Abstracts

MAGYAR K, RIBA A, VAMOS Z, BALOGH A, <u>DERES L</u>, HIDEG K, SUMEGI B, KOLLER A, HALMOSI R, TOTH K; The role of Akt and mitogen-activated protein kinase systems in the vasoprotection elicited by PARP inhibition in hypertensive rats; Paris, France, 2011.08.27. 2011. *Congress of the European Society of Cardiology, August 27-31, 2011, Paris, France [EHJ, Abstract Suppl.]*

MAGYAR K, RIBA A, VÁMOS Z, BALOGH A, <u>DERES L</u>, KÁLAI T, HIDEG K, SERESS L, SÜMEGI B, KOLLER A, HALMOSI R, TÓTH K; The role of akt and mitogen-activated protein kinase systems in the protective effect of parp inhibition in a chronic hypertensive rat model; Magyar Farmakológiai, Anatómus, Mikrocirkulációs és Élettani (FAMÉ) társaságok 2011. évi közös tudományos konferenciája. Pécs, Magyarország, 2011.06.08-2011.06.11. (Magyar Élettani Társaság) Pécs: *pp. 200-201.*

VÁMOS Z, CSÉPLŐ P, <u>DERES L</u>, IVIC I, KÓSA D, MÁTICS R, HAMAR J, KOLLER A Aging alters Angiotensin-II-induced vasomotor responses. Osijek, Croatia, 2011.09.24. 2011. *Croatian Physiological Society Meeting, Osijek, sept. 24-25., 2011.*

VAMOS Z, CSEPLO P, <u>DERES L</u>, HAMAR J, KOLLER A Aging dependent changes in angiotensin II-induced contractions of isolated rat carotid atreries. München, Németország, 2011.10.11-2011.10.18. 2011. *Meeting of the European Society for Microcirculation, München, okt. 11-18.,2011.*

VÁMOS Z, CSÉPLŐ P, KÓSA D, <u>DERES L</u>, IVIC I, HAMAR J, KOLLER A; Aging alters angiotensin II - induced vasomotor responses. Correlation with changes in AT_1-receptor expression. *Hypertonia és nephrologia* 15:(S3) *p. 44.* (2011) *Magyar Hypertonia Társaság XIX. Kongresszusa Budapest, Magyarország, 2011.11.30-2011.12.03.*

<u>DERES L</u>, MAGYAR K, TAKÁCS I, ERŐS K, BALOGH A, HIDEG K, SÜMEGI B, TÓTH K, HALMOSI R; Pharmacological PARP-inhibition decreases vascular fibrosis in spontaneously hypertensive rat model; Balatonfüred, Magyarország, 2012.05.09-2012.05.12. 2012. *Congress of Hungarian Society of Cardiology 2012. Balatonfüred, Cardiologia Hungarica 2012; 42:A21*

<u>DERES L</u>, VÁMOS Z, ERŐS K, MÁTICS R, CSÉPLŐ P, HALMOSI R, SÜMEGI B, TÓTH K, KOLLER A; Subcellular aspects of AT1-receptor mediated vasomotor responses in relation to age; Balatonfüred, Magyarország, 2013.05.08. 2013. *Congress of Hungarian Society of Cardiology 2013. Balatonfüred, Cardiologia Hungarica 2013; 43:B16*

ERŐS K, <u>DERES L</u>, MAGYAR K, RIBA Á, HIDEG K, SERESS L, SÜMEGI B, TÓTH K, HALMOSI R; Effect of PARP-1 inhibition on the mitochondrial fragmentation in an *in vivo* SHR model; Balatonfüred, Hungary, 2013. *Congress of Hungarian Society of Cardiology 2013. Balatonfüred, Cardiologia Hungarica 2013; 43:B16*

VÁMOS Z, <u>DERES L</u>, ERŐS K, MÁTICS R, IVIC I, BERTALAN A, SIPOS E, KOLLER A, CSÉPLŐ P; Aging alters angiotensin II - induced vasomotor responses. Correlation with changes in AT_1-receptor expression. Balatonfüred, Hungary, 2013. *Congress of Hungarian Society of Cardiology 2013. Balatonfüred, Cardiologia Hungarica 2013; 43:B32*

EROS K, <u>DERES L</u>, MAGYAR K, RIBA A, HIDEG K, SERESS L, SUMEGI B, TOTH K, HALMOSI R; Effect of PARP-1 Inhibition on the Mitochondrial Fragmentation in an in vivo SHR Model. *VII. International Symposium on Myocardial Cytoprotection 2013 Pecs, Hungary. Cardiologia Hungarica 2013; 43:G13*

HALMOSI R, <u>DERES L</u>, EROS K, MAGYAR K, BARTHA E, TAKACS A, KALAI T, SERESS L, GALLYAS F, SUMEGI B, TOTH K; The Protective Effect of PARP-inhibitors Against Hypertension Induced Myocardial and Vascular Remodeling. *VII. International Symposium on Myocardial Cytoprotection 2013 Pecs, Hungary. Cardiologia Hungarica 2013; 43:G15*

MAGYAR K, TAKACS A, <u>DERES L</u>, EROS K, SERESS L, VAMOS Z, HIDEG K, KALAI T, BALOGH A, KOLLER A, SUMEGI B, TOTH K, HALMOSI R; Pharmacological inhibition of PARP-1 Enzyme Prevents Hypertensive Vascular Remodeling. *VII. International Symposium on Myocardial Cytoprotection 2013 Pecs, Hungary. Cardiologia Hungarica 2013; 43:G20*

<u>DERES L</u>, EROS K, BENCZE N, SERESS L, SUMEGI B, FARKAS S, TOTH K, HALMOSI R; The effects of a bradykinin B1 receptor antagonist on the development of hypertensive organ damages; Balatonfüred, Hungary, 2014. *Congress of Hungarian Society of Cardiology 2014. Balatonfüred, Cardiologia Hungarica 2014; 44:E25*

VAMOS Z, CSEPLO P, DERES L, SETALO GY Jr, MATICS R, KOLLER A; Age dependent changes in subcellular mechanism responsible for AT1-receptor mediated vasoconstriction; Balatonfüred, Hungary, 2014. *Congress of Hungarian Society of Cardiology 2014. Balatonfüred, Cardiologia Hungarica 2014;44:E40*

EROS K, BARTHA E, DERES L, RIBA A, KALAI T, HIDEG K, SUMEGI B, TOTH K, HALMOSI R; Effect of poly(ADP-ribose)polymerase-1 inhibition on myocardial remodeling in a chronic hypertensive rat model; Hungary, 2014. *Congress of Hungarian Society of Cardiology 2014. Balatonfüred, Cardiologia Hungarica 2014;44:E51*

DERES L, EROS K, BENCZE N, SERESS L, SUMEGI B, FARKAS S, TOTH K, HALMOSI R; The effects of a bradykinin b1 receptor antagonist on the development of hypertensive organ damages in SHR model; *Barcelona, Spain, Congress of the European Society of Cardiology 30. August to 0.3 September 2014.*